![Cambridge University Press logo]

Geology and microstructural evolution of syn- to late-tectonic granitoids from Capo Vaticano Promontory (southern Calabria, Italy)

Damiano Russo[1] , Patrizia Fiannacca[1], Eugenio Fazio[1], Rosolino Cirrincione[1] and Manish A. Mamtani[2]

[1]Dipartimento di Scienze Biologiche, Geologiche e Ambientali, Università di Catania, Catania, Italy and [2]Indian Institute of Technology Kharagpur, Kharagpur, India

Abstract

This study presents new field and microstructural constraints into the batholith architecture and supra- to subsolidus evolution of late Variscan granitoids at Capo Vaticano Promontory, part of the ~13 km-thick Serre Batholith in southern Italy. A field survey, assisted by petrographic analyses, produced the first geological map of the area (1:140,000 scale), detailing magmatic unit relationships and their petro-structural features. A migmatitic border zone (MBZ) marks the transition from lower-crustal paragneisses to the deepest emplaced granitoids. The oldest, deepest granitoids are strongly to moderately foliated amphibole-biotite tonalites and quartz diorites, transitioning to biotite tonalites and quartz-diorites (BT), which can be subdivided into strongly to moderately foliated (BT_s) and weakly foliated to unfoliated (BT_w). Clear intrusive contacts mark the passage from BT_w to overlying weakly foliated-unfoliated porphyritic muscovite-biotite granodiorites and granites (PMBG). The study also revealed: a) a northern sector with a continuous batholith cross-section and b) a southern sector with an irregular distribution of the magmatic units due to post-Variscan tectonics. Microstructures document late Variscan deformation starting at suprasolidus conditions (e.g., quartz chessboard patterns and submagmatic fractures in plagioclase) and evolving through progressively high- to low-temperature subsolidus stages (e.g., feldspar bulging, quartz recrystallization, mica kinking) for all the magmatic units. Continuous supra- to subsolidus deformation associated with a well-developed fabric suggests tectonic control on the emplacement and cooling of early tonalites/quartz diorites, while the emplacement of the porphyritic granitoids has occurred during waning tectonic activity stages in the framework of the post-collisional evolution of the south-western Variscan Belt.

1. Introduction

It is widely accepted that extraction, ascent and emplacement of granite magmas and regional tectonics may be coeval and interdependent processes (e.g., Brown & Solar, 1999; Vigneresse, 1999; Vigneresse & Clemens, 2000; Petford & Clemens, 2000; Demartis *et al.*, 2011; Brown, 2013; Cruden & Weinberg, 2018). Valuable information on the regional strain field can be stored in the structure of granitoid rocks, from map to the microscopic scale. Fabric investigations represent, therefore, a necessary step in the study of the relationships between pluton emplacement and regional tectonics (e.g., Bouchez & Diot, 1990; Schulmann *et al.*, 1996; Zibra *et al.*, 2012; Žák *et al.*, 2012; Fazio *et al.*, 2020; Fiannacca *et al.*, 2021).

In southern Europe, the convergence between Gondwana, Gondwana-derived terranes and Laurussia led to the amalgamation of Pangea at ca. 300 Ma (Behr *et al.*, 1984; Matte, 1986; Burg *et al.*, 1987; von Raumer *et al.*, 2002, 2003, 2013). The latest Variscan stages (ca. 320–280 Ma) were characterized by coeval transpressional and transtensional tectonics, producing a complex pattern of large-scale shear zones, with associated extensive crustal melting and granitoid magmatism in the southern Variscides (Elter *et al.*, 2020; and references therein). One such shear zones was the East Variscan Shear Zone (EVSZ; Carosi *et al.*, 2020; Corsini & Rolland, 2009; Padovano *et al.*, 2012, 2014), considered as the western boundary between the peri-Gondwana microcontinents and Gondwana (e.g., Elter *et al.*, 2020), which involved various Variscan massifs dispersed throughout the western Mediterranean region. The Calabria-Peloritani Orogen (CPO; Cirrincione *et al.*, 2015, and references therein; Fig. 1a and 1b), in southern Italy, was also involved in the EVSZ, whose activity led to the development of regional mylonitic foliations, locally associated with exhumation of deep-middle crust and syn- to late-tectonic emplacement of large volumes of granitoids (Padovano *et al.*, 2012, 2014).

Remnants of the European Variscan Belt and evidence of such late Variscan crustal dynamics are well preserved in the CPO, which represents an arcuate Alpine mountain belt in southern Italy. In particular, within the CPO, the Serre Batholith (ca. 297–292 Ma; Fiannacca *et al.*, 2017,
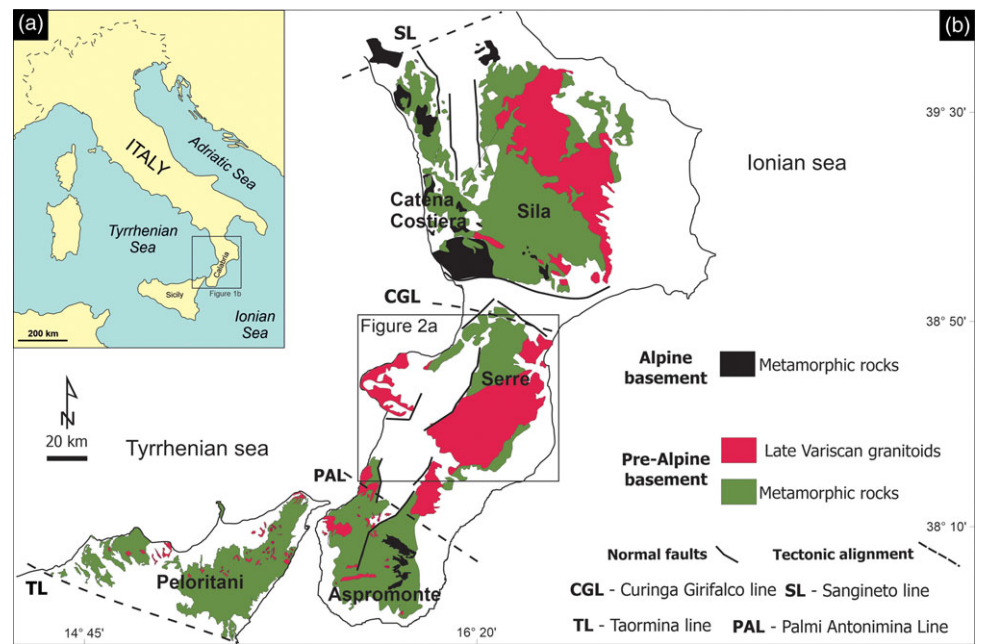
Figure 1. (a) Location of the Calabria-Peloritani Orogen (CPO) in Italy. (b) Distribution of Alpine and pre-Alpine (Variscan and/or pre-Variscan) basements in the CPO and main tectonic lineaments (modified after Angì *et al.*, 2010).

and references therein), in southern Calabria (Fig. 2a), is a ca. 13 km-thick composite and zoned batholith, forming the intermediate portion of a nearly complete and continuous cross-section of late Paleozoic continental crust (Fig. 2b). In this region, therefore, it is possible to investigate the regional processes and dynamics involved in the structuring of such outstanding Variscan crustal section.

Specifically, this study focuses on the relationships between solidification-cooling and deformation of the granitoids that make up the deepest levels of the Serre Batholith, by investigating quartz diorites-tonalites and porphyritic two-mica granodiorites-granites exposed in the Capo Vaticano Promontory (CVP). In this framework, a detailed field survey was first carried out in order to map the different granitoid units, distinguishing their specific petrographic and structural features, and investigate the relationships between them, highlighting the architecture of the granitoid complex. In addition, field studies allowed realizing the first detailed geological map of the magmatic units from the CVP. Finally, this work presents a study of the microstructural evolution from magmatic to low-temperature subsolidus conditions of the studied rocks, able, for the first time, to depict the late Variscan deformation history of this sector of the Serre Batholith.

2. Geological setting

2.a. The Serre Massif

The Serre Massif (Fig. 2a) is a natural laboratory where a ca. 25 km-thick cross-section of late Paleozoic continental crust is exposed with continuity from upper crustal phyllites to deep crustal granulites (Schenk, 1981, 1990; Caggianelli *et al.*, 2007; Angì *et al.*, 2010). Mafic granulites including layered metagabbros make up the lowermost crustal levels (ca. 3 km-thick) together with minor felsic granulites, fine-grained metapelites and metacarbonates, and are overlain by a metapelitic migmatitic complex (ca. 4 km-thick) mostly consisting of migmatitic paragneisses, and minor intercalated metabasites and metacarbonates (Schenk, 1980, 1984).

The mafic granulites from the base of the crustal section experienced peak PT conditions of at least 1.1 GPa at 900°C (Fornelli *et al.*, 2012; and references therein). Thickening-related peak P conditions up to 0.9 GPa at ~ 650°C, followed by prolonged nearly isobaric heating up to peak temperatures of ~ 700°C, have been indicated by the same authors for the migmatitic metapelites from the top of the lower crust.

The intermediate crustal segment is represented by the Serre Batholith, a ca. 13 km-thick composite and zoned batholith (e.g., Rottura *et al.*, 1990; Caggianelli *et al.*, 2000a, b; Fornelli *et al.*, 1994; Fiannacca *et al.* 2015, 2017). Granitoids were produced by melting of different crustal magma sources (Fiannacca *et al.*, 2015; and references therein), and emplaced at depths between ~23 and ~6 km (Al-in-hornblende barometry, Caggianelli *et al.*, 1997). The batholith is built up through an incremental over-accretion mechanism, with the magmas emplaced at progressively decreasing depths (Fiannacca *et al.*, 2017; and references therein). Strongly to moderately foliated tonalites and quartz diorites were emplaced first, at lower-crustal levels (ca. 297 Ma, at ca. 6.5 kbar) forming the batholith floor; they were followed upward by intermediate-seated weakly foliated to non-foliated porphyritic two mica granodiorites and granites (ca. 296-295 Ma) and, finally, by locally foliated equigranular two mica granodiorites and granites (ca. 294 Ma) and biotite ± amphibole granodiorites (ca. 292 Ma, at ca. 1.7 kbar), the latter forming the batholith roof. Taking into account the U-Pb zircon SHRIMP analytical errors, these results indicate that the Serre Batholith may have been formed over a relatively short period of ca 5 Ma and, anyway, not greater than 9 Ma (Fiannacca *et al.*, 2017).

The uppermost crustal segment is made up of two metamorphic complexes (ca. 2–3 km thick), the Mammola Paragneiss Complex and the overlying Stilo-Pazzano Complex, juxtaposed along a low angle tectonic detachment before the intrusion of the Serre Batholith granitoids (Colonna *et al.*, 1973; Angì *et al.*, 2010; Festa *et al.*, 2013; Ortolano *et al.*, 2022). The Mammola complex includes dominant upper greenschist to amphibolite-facies paragneisses with subordinate leucocratic gneisses and amphibolites.
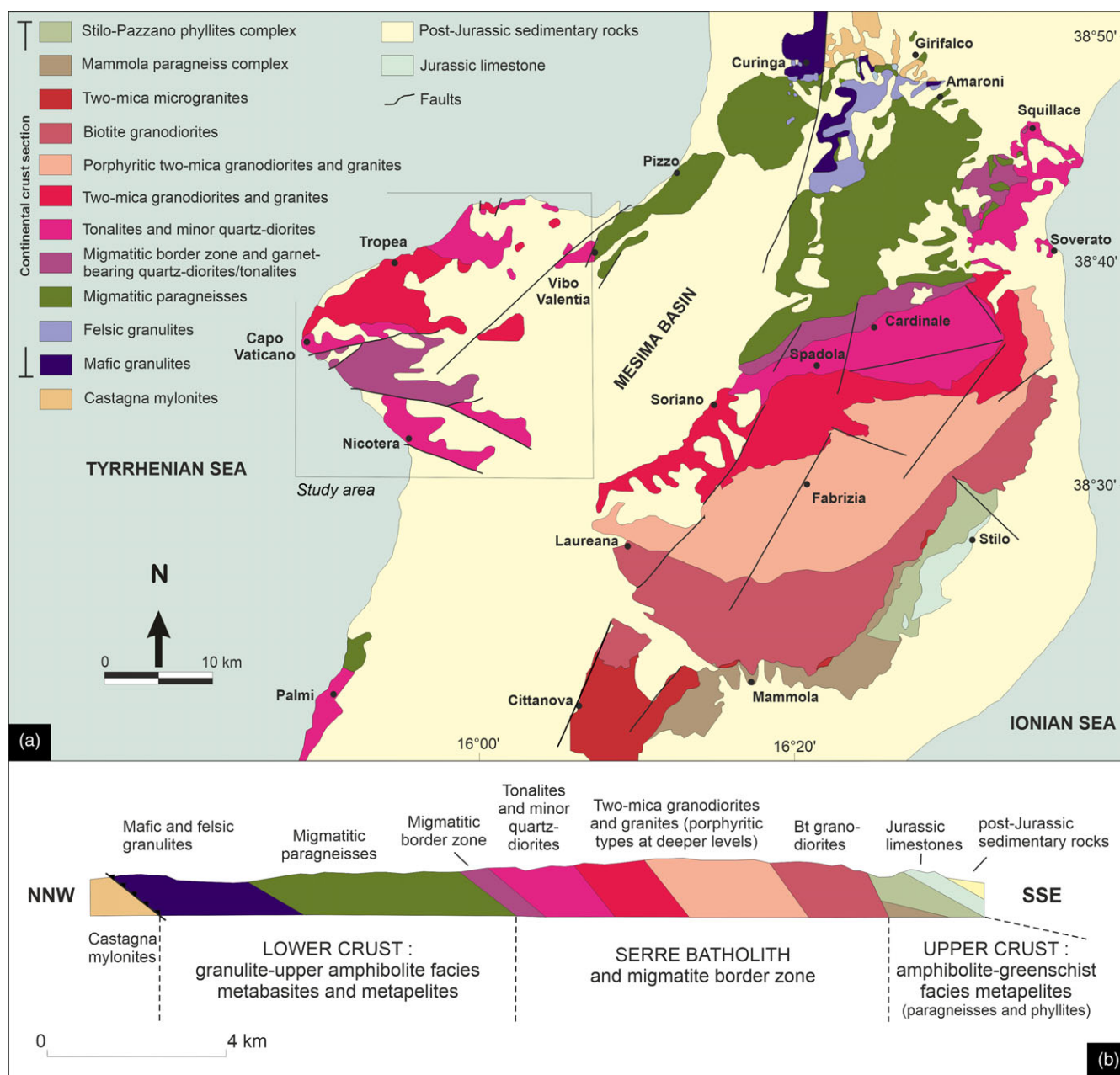
Figure 2. (a) Geological sketch map of the Serre Massif and Capo Vaticano Promontory area (modified after Russo *et al.*, 2023 and references therein); (b) Simplified lithological cross-section of the Serre Massif (modified after Fiannacca *et al.*, 2015 and references therein).

The Stilo-Pazzano complex is mainly represented by lower greenschist-facies phyllites with minor marbles, quartzites and metavolcanic layers, with protolith ages possibly ranging from the Cambro-Ordovician to the Carboniferous (Navas-Parejo *et al.*, 2015; and references therein). Both complexes share the same static metamorphic overprint as a result of the emplacement of the late Variscan granitoids (Ortolano *et al.*, 2022; and references therein). Before experiencing contact metamorphism, the upper crustal Mammola paragneisses underwent an initial deformational stage (D_1), characterized by the formation of a penetrative and pervasive surface (S_1). D_1 was followed by a D_2 crenulation stage producing a S_2 crenulation cleavage. These two prograde stages, consistent with eo-Variscan crustal thickening stage, were followed by a near-isothermal decompression path, consistent with tectonic transport

along a dominant extensional shear zone, leading to the development of a pervasive mylonitic foliation (S3) and likely assisting the emplacement of the granitoid magmas (Angì *et al.*, 2010). In particular, according to the above authors, Mammola paragneisses were involved in collision-related crustal thickening together with the lower-crustal migmatitic paragneisses up to peak P–T values of 0.9 GPa at 530°C, but then rapidly detached from the lower-crustal rocks and uplifted to upper crustal levels (up to ~ 0.3 GPa at 470°C) along the above-mentioned shear zone. In this framework, Fiannacca *et al.* (2017), based on the matching of the pressure values along the decompressional path of the Mammola paragneisses with the progressively younger intrusion ages of the granitoids emplaced at progressively lower depths, proposed that the Mammola paragneisses, during their shear-related uplift,

accommodated the progressive emplacement of the late Variscan granitoid magmas; magma emplacement was associated with shear-zone activity up to the latest magmatic stages, as suggested by late-tectonic felsic dykes with clear evidence of mylonitic deformation (Angì *et al.*, 2010). A tectonic event with a 30–40% simple shear component along a sub-horizontal plane was also suggested for the late Variscan evolution of the deep crustal metapelites (Festa *et al.*, 2012). Finally, both the granitoids and the upper crustal metamorphic rocks are locally intruded by late to post-Variscan felsic to mafic dykes (Romano *et al.*, 2011).

2.b. The Capo Vaticano Promontory

The Capo Vaticano Promontory (study area, Fig. 2a), along the coast of the Tyrrhenian Sea, represents a deep-intermediate portion of the Serre Batholith that, together with its lower crustal migmatitic host rocks, was separated from the Serre Massif by the opening of Miocene-Pleistocene Mesima graben, and further dismembered by Quaternary tectonics (Tortorici *et al.*, 2003; Conforti & Ietto, 2020). Since the Middle Pleistocene, an intense ESE–WNW oriented regional extensional phase, as a consequence of the Ionian slab subduction beneath Calabria, has influenced the recent tectonic evolution of the region (Tortorici *et al.*, 2003, and references therein). In the CVP, this tectonic event led to the development of several normal faults with NE-SW and WNW-ESE dominant trends (Ghisetti & Vezzani, 1981; Monaco & Tortorici, 2000; Tortorici *et al.*, 2003; Perri *et al.*, 2016). The post-Variscan tectonic events therefore led to a large disruption of the late Variscan architecture of the lower-intermediate crust now exposed in the CVP.

The CVP granitoids extend over an area of ca. 270 km^2 (Rottura *et al.*, 1991; Lombardo *et al.*, 2020), cropping out discontinuously beneath a Miocene-Pliocene terrigenous and carbonate cover and upper Quaternary deposits (Burton, 1971; Tortorici *et al.*, 2003; Bianca *et al.*, 2011). The lower-crustal host rocks, mostly consisting of migmatitic paragneisses, crop out extensively in the north-eastern part of the CVP, in near continuity with the lower-crustal rocks extensively exposed in the northern Serre Massif, and, locally, in the south-western part, as a consequence of post-Variscan tectonics (Clarke & Rottura, 1994; Fornelli *et al.*, 2002, 2004).

The CVP granitoids consist of strongly to weakly foliated tonalites and minor quartz diorites, which account for ca. 65% of the exposed magmatic rocks, and weakly to non-foliated porphyritic granodiorites, with fewer granites (ca. 35%). According to Caggianelli *et al.* (1991) and Rottura *et al.* (1990, 1991), strongly foliated tonalites and quartz diorites were intruded earlier into the lower-crustal gneisses, locally triggering extensive further partial melting in the already anatectic country rocks, with development of a migmatitic border zone (MBZ) (Clarke & Rottura, 1994), while weakly foliated tonalites and granodiorites were intruded later, at progressively shallower crustal levels. Nevertheless, recent U-Pb SHRIMP zircon dating of strongly to weakly foliated tonalites and quartz diorites indicates a similar age of ca. 299–297 Ma for all the deepest granitoids (Lombardo, 2020). According to Al-in-hornblende barometric estimates by Caggianelli *et al.* (1997, 2000b), the CVP tonalites-quartz diorites were distinguished into intermediate crust granitoids, emplaced at depths ranging from ca. 17.5 to 20 km (Ioppolo, Santa Maria, Capo Vaticano), and lower crust granitoids, emplaced at depths greater than ca. 20 km (Briatico). In accordance with preliminary fabric investigations, the same authors suggested that these granitoids

experienced prolonged deformation at temperature above the brittle- ductile transition, at which they resided for periods up to 100 Ma (Caggianelli *et al.*, 2000a). Granitoids vary in composition from metaluminous/weakly peraluminous quartz-diorites and tonalites, cropping out in the north and in the south of the CVP, to strongly peraluminous porphyritic granodiorites and granites in the central sector of the CVP (Fiannacca *et al.*, 2015; and references therein). No barometric or geochronological data are available for the porphyritic granitoids, but field relationships and comparison with such data obtained in the Serre Massif (Caggianelli *et al.*, 2000b; Fiannacca *et al.*, 2017) indicate that the latter rocks are both younger and shallower, consistent with an over-accretion emplacement mechanism (Fiannacca *et al.*, 2017; and references therein).

Several petrogenetic interpretations have been proposed for the CVP granitoids. Tonalites and quartz diorites have been interpreted either as resulting from the interaction of mantle-derived magmas with crustal rocks (Rottura *et al.*, 1991) or as I-type granitoids derived from partial melting of a mafic lower-crustal source (Rottura *et al.*, 1990; Fiannacca *et al.*, 2015). The strongly peraluminous granitoids have been interpreted as the result of mixing between two distinct felsic melts, one of crustal origin and the other derived from the CVP tonalitic magma through fractional crystallization or assimilation-fractional crystallization (Rottura *et al.*, 1991), or as typical S-type granites (e.g., Rottura *et al.*, 1990; Fiannacca *et al.*, 2015). For both granitoid types, fractional crystallization has been proposed by Lombardo *et al.* (2020) as the main process responsible for magmatic evolution from quartz diorite to tonalite and from granodiorite to granite, respectively.

3. Materials and methods

Petro-structural studies were conducted on thin sections of 52 pre-existing samples (Fiannacca *et al.*, 2015; Lombardo, 2020) and 30 newly acquired ones from the study area and analyzed with an Axioscope 2 optical microscope (Zeiss, Germany). Crossed polar images of entire thin sections of representative samples were acquired by using a flatbed scanner (Epson Perfection 3490 Photo; Seiko, Japan) at a resolution of 4800 dpi, together with several photomicrographs of deformed domains taken by a Leica ICC50W Camera (Leica Microsystems, Switzerland) mounted on the Leica DM750P Microscope, both hosted at the Department of Biological, Geological and Environmental Sciences, University of Catania. Abbreviations for the different mineral phases are after Whitney & Evans (2010).

4. Geological mapping and design

A geological map of the magmatic units exposed in Capo Vaticano Promontory is presented for the first time in this study (Fig. 3). Mapping also included the MBZ developed at the contact between the deepest granitoids and the lower-crustal host rocks in the southern sector of the CVP. The surveyed area is approximately 150 km^2, at a scale of 1:140,000. Geological survey has been performed using the 1:50,000 topographic maps of the Istituto Geografico Militare and digitalized by means of the ArcGIS® software. Field data and sampling locations were stored in a georeferenced geological database built in WGS 1984 UTM zone 33N reference system. A topographic dataset, available in vector format at 'Geoportale della Regione Calabria' website (http://geoportale.regione.calabria.it), has been employed as topographic base
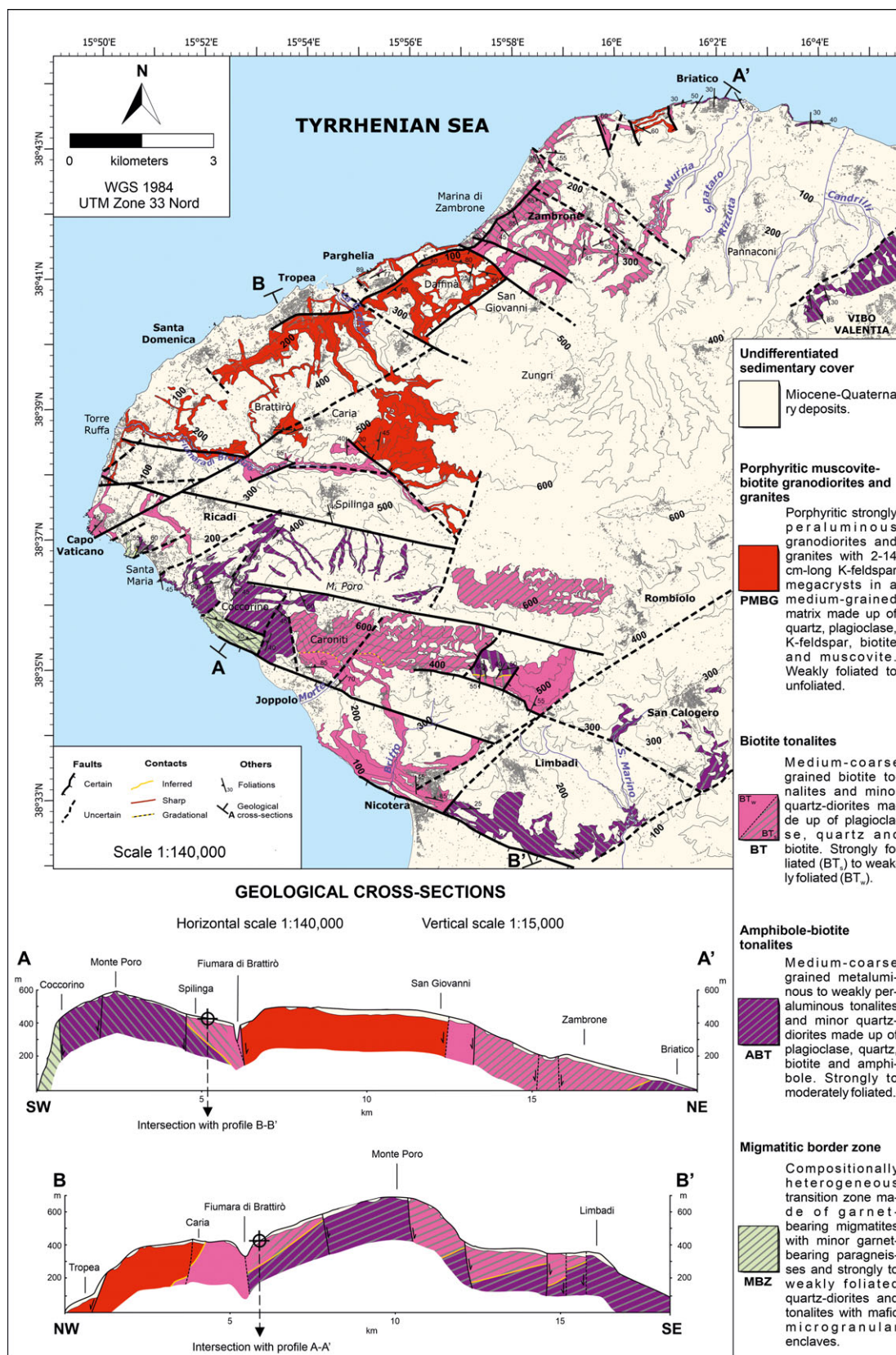
Figure 3. Petro-structural map of the magmatic units exposed in the Capo Vaticano Promontory (southern Calabria, Italy). The displayed patterns represent the average foliation of the strongly to moderately foliated granitoids.

for the geological map. Final assemblage and graphical editing have been realized with CorelDRAW® software on a vector PDF file exported from ArcGIS®. The geological-structural map is the result of an accurate field survey integrated with mesoscopic and microscopic investigations, allowing us to delineate the main field and petrographic features of the Capo Vaticano Promontory granitoids. The official geological map of the area (Cassa per il Mezzogiorno - Servizio Geologico d'Italia, 1967), at a scale of 1:25,000, which is available online (http://geoportale.regione.cala bria.it/opendata) as georeferenced TIFF files, was used as initial reference for the purposes of this study. However, the latter identifies a single plutonic unit, without compositional and structural distinctions between the different granitoids cropping out in the area. Other information on the spatial distribution of the mapped rocks appears in Rottura *et al.* (1991), although only consisting of a sketch map with no description of the field relationships between the depicted units. The widespread sedimentary rocks have been collectively represented as undiffer-entiated Miocene-Quaternary sedimentary cover.

5. Granitoids from the Capo Vaticano Promontory

Granitoid outcrops in Capo Vaticano Promontory are better exposed in the coastal areas and along riverbeds; in the inland areas they mostly occur in sectors bounded by faults. Tonalites-quartz diorites are strongly or moderately foliated in the northern and southern part of the study area, while they are weakly to non-foliated in the central part, where they are intruded by the overlying porphyritic granitoids, and, locally in some areas of the southern sector. In this section, we report the main field and petrographic features of the granitoids units that make up the CVP, which, are reported following the criteria and terminology already used by Russo *et al.* (2023; and references therein) for the north-eastern sector on the Serre Batholith, in the Serre Massif (Fig. 2). The main field features of the MBZ are also reported in this section; more details can be found in Fiannacca *et al.* (2024; and references therein).

5.a. Migmatitic border zone (MBZ)

The MBZ is exposed in scattered areas of a few square kilometres each in the south-western sector of CVP. The unit represents a transition zone between the top of the metamorphic lower-crustal section and the earliest and deepest emplaced granitoids of the Serre Batholith, i.e., the tonalites/quartz diorites (hereafter 'tonalites' for brevity, since tonalites are the dominant rock type). The MBZ is characterized by: a) migmatitic paragneisses ranging from metatexites to diatexites with a highly irregular distribution and abundance of leucosomes and peritectic garnets, and b) medium-coarse-grained tonalites including abundant cm- to m-sized metapelitic enclaves, as well as large crystals of peritectic garnet. The latter, typically 1–2 cm in size, is mainly associated with the metapelitic enclaves, occurring in extremely variable amounts in cm- to m-sized leucosome patches, but also present as isolated crystals in tonalites far away from the enclaves. This peculiar multiscale commixture of tonalites, metapelitic enclaves and associated garnet-bearing leucosomes, also documented in the northern Serre Massif (Rottura *et al.*, 1990; Russo *et al.*, 2023), resulted from the interaction between the intruding tonalite magma and the anatectic magmas produced by extensive further melting of the already migmatitic hosting paragneisses

(Clarke & Rottura, 1994). Typical features of the MBZ outcrops are illustrated in Fig. 4a–4e.

5.b. Amphibole-biotite tonalites (ABT)

Amphibole-biotite tonalites and quartz diorites (ABT) are mainly exposed in the southern sector of the CVP over a total area of ca. 17 km², in a ca. 3 km² body in the north-eastern sector, and in a ca. 2 km-long and ca. 80 m-wide band running along the northern coast of the CVP. They are medium-coarse-grained rocks, strongly to moderately foliated and rich in elongated mafic microgranular enclaves parallel to host rock foliation (Fig. 5a–5c). In some cases, mafic microgranular enclaves exhibit a monoclinic symmetry indicating that they have recorded a component of non-coaxial deformation (Fig. 5d). In the southwestern sector of the studied area, a compositional layering, represented by an alternation of cm-thick more felsic and more mafic layers, locally occurs. Cm- to m- thick pegmatitic and aplitic dykes are widespread. Texture is generally sub-hypidiomorphic and commonly cumulitic, defined by a compact framework of euhedral-subhedral plagioclase crystals with subhedral amphibole and interstitial biotite, quartz and epidote (Fig. 6a and 6b). Colour index is in the range 25–40. ABT is made up of unzoned to weakly zoned euhedral to subhedral plagioclase (ca. 50 vol. %), subhedral to anhedral biotite (ca. 28 vol. %) as isolated individuals or in clots, quartz (ca. 17 vol. %) in anhedral crystals and amphibole (ca. 5 vol. %) as subhedral to anhedral crystals, occasionally partly replaced by biotite. Epidote, titanite, allanite, apatite, ilmenite and zircon are the main accessories.

5.c. Biotite tonalites (BT)

Biotite tonalites and minor quartz diorites (BT) are the most widespread rock types in the CVP, outcropping mostly in the north and in the south of the mapped area and covering an area of ca. 29 km². BTs are medium-coarse-grained rocks, strongly to moderately foliated (BT$_s$; Figs. 5e, 6c and 6d) or weakly to non-foliated (BT$_w$; Figs. 5f, 6e and 6f). Cm- to m-long mafic microgranular enclaves, from elongate (BT$_s$) to globular (BT$_w$) in shape, are frequently found within these rocks (Fig. 5e and 5f). Colour index is in the range 20–40. Texture is generally sub-hypidiomorphic and locally cumulitic. Colour index is in the range 20–35. All the BTs are composed of unzoned to weakly zoned euhedral to subhedral plagioclase (ca. 55 vol. %), biotite (ca. 23 vol. %), usually in clots but also as large individual crystals in the BT$_w$ and anhedral quartz (ca. 22 vol. %) (Fig. 6d and 6f). Biotite occurs in aggregates and isolated plates or, locally, as larger prismatic crystals, possibly pseudomorphic on pre-existing amphibole. Primary muscovite rarely occurs as small interstitial crystals, typically associated with biotite, in the more evolved rocks. Ilmenite, allanite, titanite, epidote, apatite, zircon are accessories. Pegmatitic and aplitic dykes are widespread and particularly abundant in the BT$_w$.

5.d. Porphyritic muscovite-biotite granodiorites and granites (PMBG)

Porphyritic muscovite-biotite granodiorites and granites (PMBG) occupy the central sector of the CVP over an area of ca. 15 km². They are porphyritic due to the presence of K-feldspar phenocrysts and megacrysts from 2 to 14 cm in length, in a medium- to coarse-grained matrix made of quartz, plagioclase, K-feldspar and biotite (Figs. 6g, 6h and 7a–7c). Locally, rough alignments of the
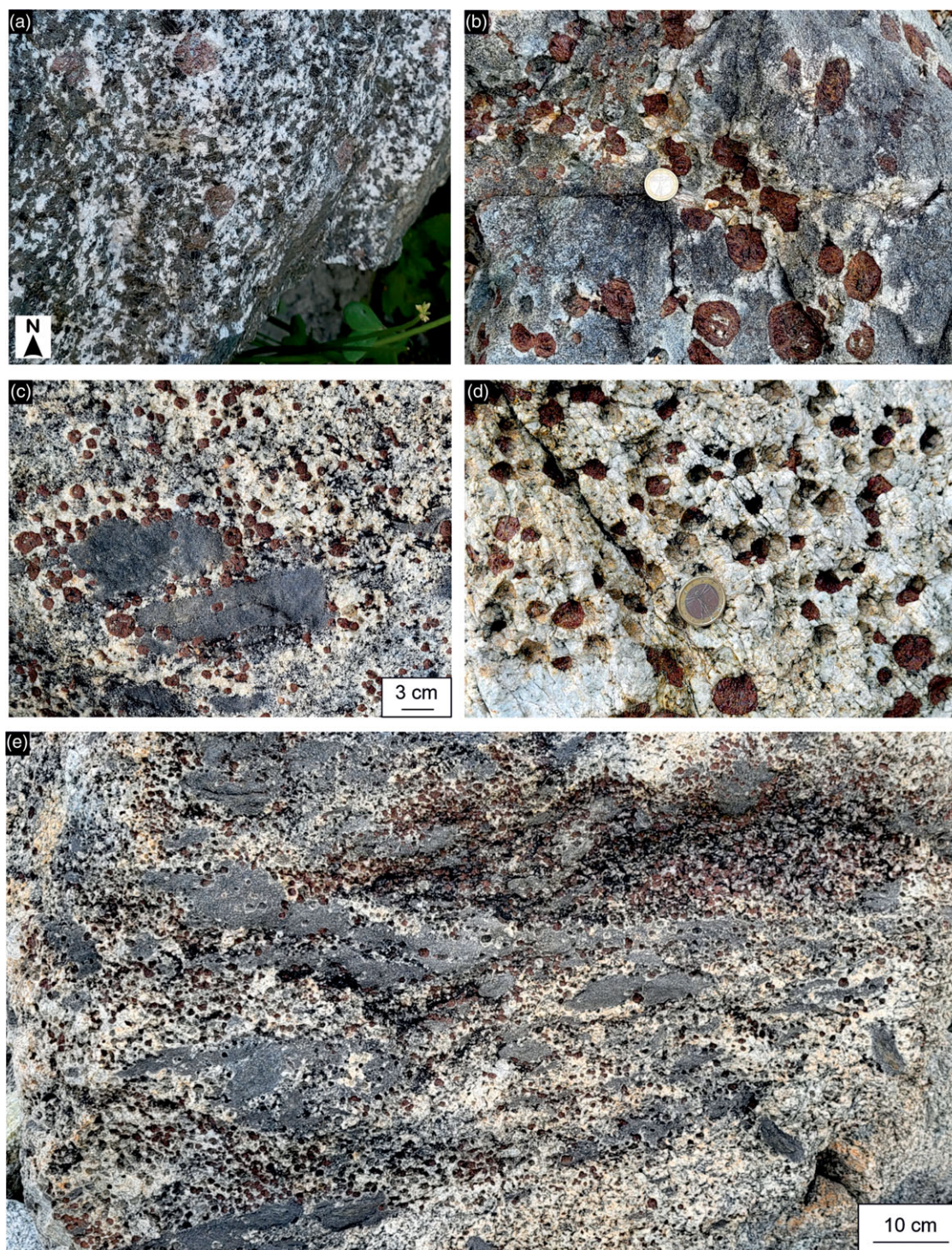
Figure 4. Interaction between tonalitic/quartz dioritic magma and the metapelitic basement in the Migmatitic Border Zone. (a) garnet-bearing quartz diorite; the largest garnet is 2.4 cm (38°35′29″ N 15°53′02″ E). (b) garnet-rich coalescing leucosome channels in migmatitic paragneiss (38°36′45″ N, 15°50′34″ E). (c) garnet-rich leucosomes bordering metapelitic enclaves rounded by consumption upon melting; the longest enclave is 15 cm long (38°36′45″ N, 15°50′34″ E). (d) typical garnet-rich anatectic rock from the MBZ (38°36′45″ N, 15°50′34″ E). (e) migmatite outcrop with metapelitic restites forming aligned enclaves in leucosomes variably enriched in large peritectic garnet (38°36′45″ N, 15°50′34″ E).

K-feldspar megacrysts and biotite plates define a magmatic foliation. A direct relationship between depth and frequency of K-feldspar megacrysts has been registered, moving from the northernmost sector, representing the deepest levels of the unit, in primary contact with the underlying BT. K-feldspar crystals reach their maximum length of 14 cm near Parghelia village, but crystals up to 7 cm long have been found also near Daffinà village with an average length of 3–4 cm. In the southern area, the average K-feldspar phenocryst length is estimated at about 1–2 cm, with the maximum length (up to 4 cm) recorded close to Brattirò village. Furthermore, in accordance with the spatial density analysis of K-feldspar megacrysts in the Serre Massif by Russo *et al.* (2023),
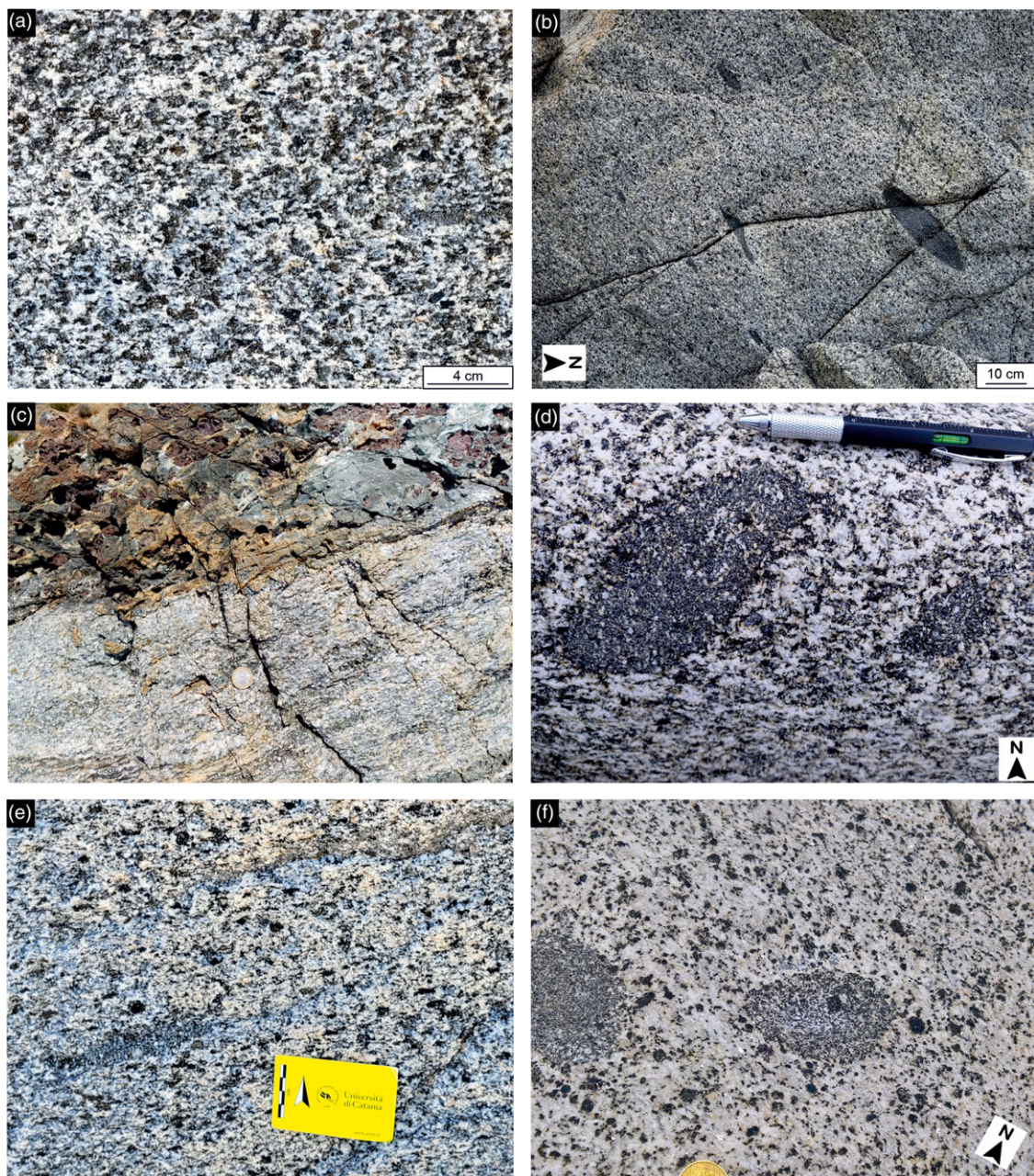
Figure 5. Characteristic field appearance of the amphibole-biotite tonalites and quartz diorites-biotite tonalites and minor quartz diorites (ABT-BT) from the Capo Vaticano Promontory area. (a) Moderately foliated ABT (38°43′38″ N, 16°01′45″ E). (b) Swarms of stretched mafic microgranular enclaves in ABT (38°36′23″ N 15°51′00″ E). (c) Sharp intrusive contact between the lower-crustal migmatitic paragneisses and the strongly foliated tonalites from the batholith floor (38°36′45″N 15°50′23″E). (d) Fish-shaped mafic microgranular enclaves in ABT (38°43′38″ N, 16°01′45″ E). (e) Moderately foliated BTs with flattened mafic microgranular enclaves (38°42′44″ N, 15°58′40″ E). (f) Unfoliated BT$_w$ with ellipsoidal MME (38°41′07″ N, 15°55′15″ E).

megacrysts occurrence registers a gradual drop from the lower to the upper levels of the PMBG unit; the maximum density is measured in the northern sector where ca. 100–120 megacrysts/m^2 occur; on the other hand, in the southern region a minimum of ca. 20–40 megacrysts/m^2 is registered. Matrix is generally hypidiomorphic and consists of perthitic microcline and, more rarely, orthoclase (ca. 35 vol %), anhedral quartz (ca. 30 vol %), subhedral plagioclase (ca. 25 vol %), subhedral-anhedral biotite (ca. 5 vol %), and subhedral-anhedral muscovite (ca. 5 vol %), mainly bordering K-feldspar and quartz or intergrown with biotite (Fig. 6h). Apatite,

zircon, ilmenite and monazite occur as accessory phases, frequently in association with biotite. Small poikilitic garnet is very locally found. Colour index is in the range 7–15. Cm- to m-thick aplitic and pegmatitic dykes occur locally.

6. Field relationships between granitoids units

In the CVP, magmatic contacts are very rarely exposed and the relationships between granitoid units cannot be clearly defined, especially in the inland areas due to large sedimentary and
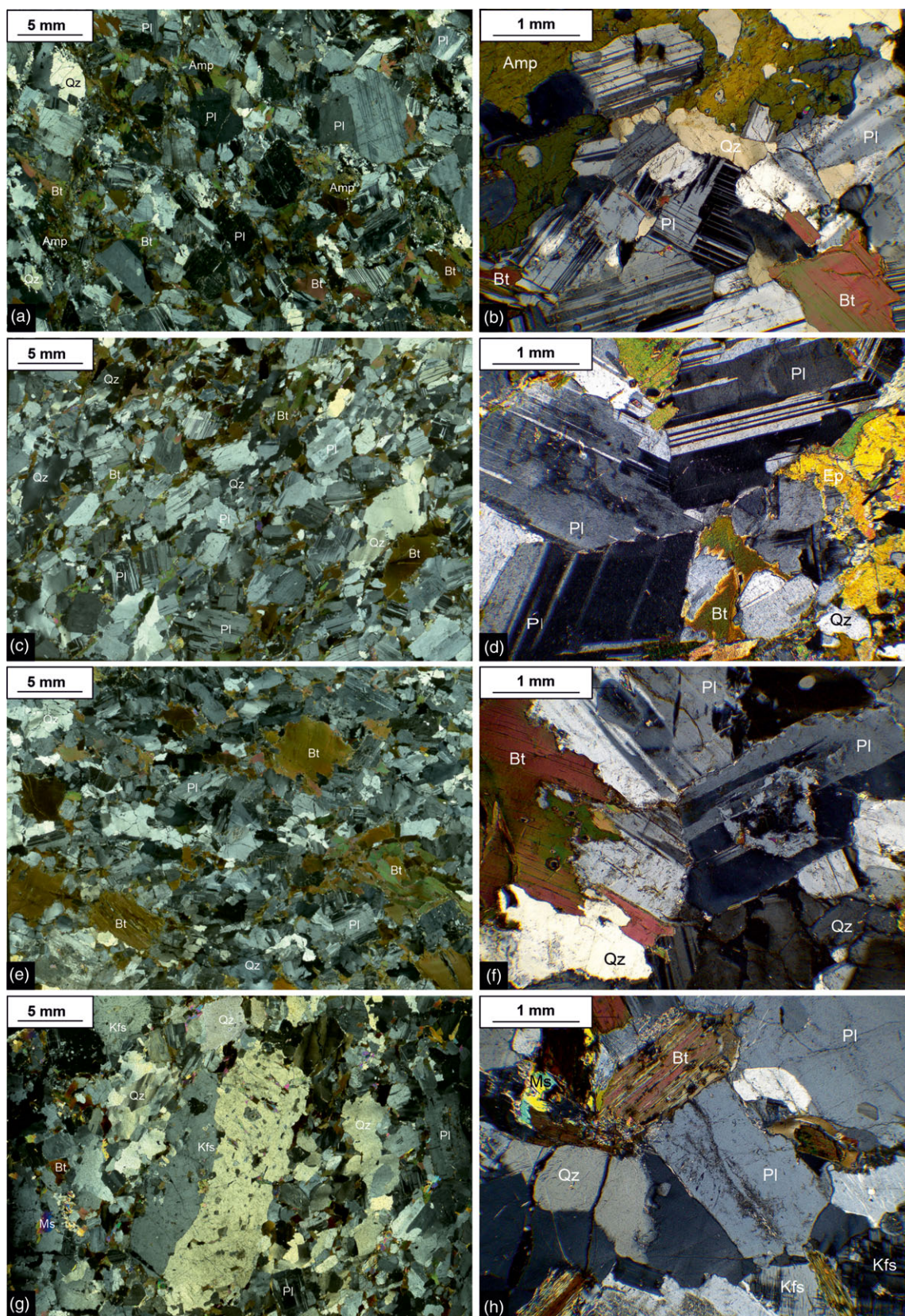
Figure 6. General petrographic features of the studied granitoids (crossed polars) from thin section scans (to the left) paired with microphotographs of representative microdomains (to the right). (a, b) ABT; (c, d) BT$_s$; (e, f) BT$_w$; (g, h) PMBG.

Figure 7. Characteristic field appearance of porphyritic muscovite-biotite granodiorites and granites from the Capo Vaticano Promontory area (38°41′07″N, 15°55′15″E). (a) Euhedral K-feldspar megacryst exhibiting zoning. (b) Aligned K-feldspar megacrysts up to 6 cm long. (c) Accumulation of K-feldspar megacrysts dominantly showing simple twinning.

anthropogenic cover, as well as to the extensive post-Variscan tectonisation and associated deterioration of the outcrops that prevent fruitful observations in these zones. However, coastal and fluvial areas expose very well-preserved outcrops, which have been crucial in defining the petro-mineralogical features of the contact zones between the various lithotypes, outlined in detail below. The great majority of the contacts are by fault, and only very rare sharp intrusive contacts have been observed and mapped in Fig. 3. In other cases, we have used the term 'gradational', where the contact between two magmatic units, or sub-units, is not sharp, but consisting in a progressive change in the composition or structure of the rocks over a certain distance. As for the BT, divided into the BT_s and BT_w sub-units, the change is only structural. In contrast, between MBZ and ABT, it is both structural and compositional.

6.a. MBZ-ABT

The relationships between the MBZ and the tonalites/quartz diorites forming the floor of the Serre Batholith in the CVP sector have only been observed in a few outcrops from the SW of the promontory (Figs. 4 and 5c) where the dominant rock types are quartz diorites to quartz-poor tonalites (Clarke & Rottura, 1994; Caggianelli *et al.* 2013; Fiannacca *et al.*, 2024). Basal tonalites exhibit varying stages of interaction with garnet-bearing or garnet-free anatectic magma produced by melting of the metapelitic migmatites after intrusion of the tonalites. The typical evidence of interaction between the anatectic magma and a crystal-poor tonalitic mush is provided by the occurrence of outstanding large peritectic garnets in apparently homogeneous tonalite (Fig. 4a). In the metapelites, on the other hand, it is possible to observe highly

variable leucosome/protolith ratios reflecting different melting degrees of the metapelites. Lower melting degrees can be inferred for paragneiss-dominated migmatites with low volumes of garnet-rich leucosomes, occurring as thin layers and patches that locally connect one to each other (Fig. 4b). With increased melting, the metapelites were strongly consumed, now forming dm- to cm-sized globular enclaves, typically bordered by large peritectic garnet, in volumetrically dominant leucosome (Fig. 4c). The end-member result of the process was a garnet-rich anatectic granitoid rock (Fig. 4d) with no, or scarce and small-sized, paragneiss remnants. The amount and size of the peritectic garnet in such anatectic granitoids is also strongly variable, even at very short distances, as illustrated in Fig. 4e.

6.b. ABT-BT

The primary magmatic relationships between the ABT and BT were not directly observed in the field.

Both units typically display a medium-coarse grain size, with no observable differences close to the ABT-BT contact. Moreover, field observations reveal no direct evidence of interaction between different magmas. In most cases, the two magmatic units are juxtaposed by normal faults, related to the main tectonic lineaments of the area. However, in the very few areas of primary interaction between the two units not affected by faulting, the mesoscopic and microscopic evidence points to a gradual transition between amphibole-bearing and amphibole-free tonalites. This relationship is supported by local evidence of partial late-magmatic replacement of amphibole by biotite in the ABT (Fig. 8a and 8b). A complete replacement of the amphibole by biotite,
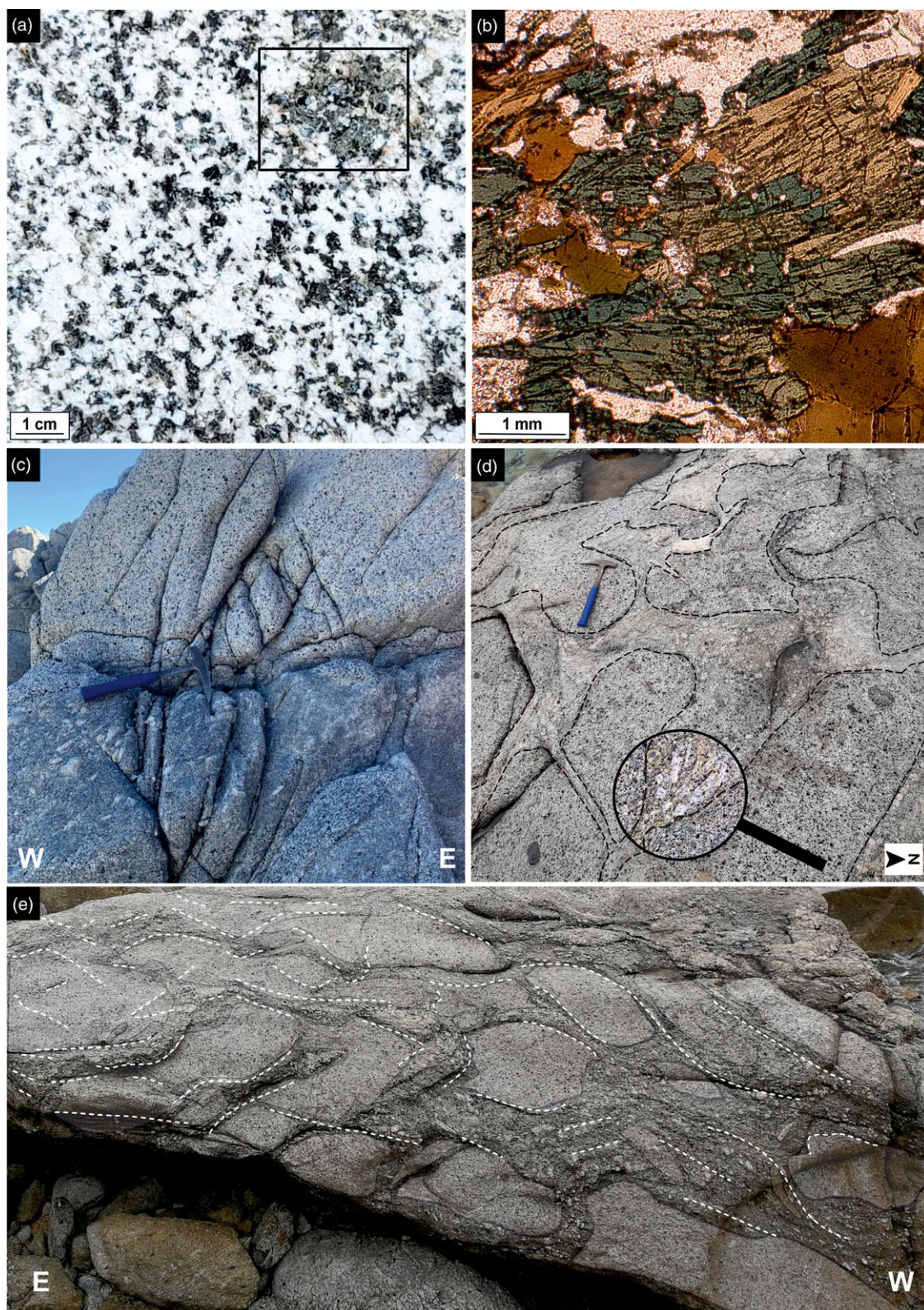
Figure 8. Relationship between the Capo Vaticano Promontory magmatic units. (a) Weakly foliated amphibole-biotite tonalites and quartz diorites (ABT) sample with large amphibole-biotite aggregates. (b) Amphibole partly replaced by biotite in ABT sample. (c) Sharp contact between biotite tonalites and minor quartz diorites (BT) and porphyritic muscovite-biotite granodiorites and granites (38°41′07″ N, 15°55′15″ E). (d) Granodioritic melt intruding into partially solidified BT, dismembering the latter in m-sized rounded blocks. Note the K-feldspar megacrysts accumulation in a filter-press-like geometry (38°41′07″ N, 15°55′15″ E). (e) Sigmoid tonalitic blocks wrapped by anastomosing granodiorites with strong magmatic fabric marked by alignment of K-feldspar megacrysts (38°41′07″ N, 15°55′15″ E).

generally preserving the shape of the original grain, is found in BT samples close to the ABT. On the other hand, biotite dominantly occurs throughout the BT unit as aggregates or single individuals with the typical tabular shape (Fig. 6c and 6e), thus suggesting a direct crystallization from the magma. These considerations would indicate an origin of the ABT and more mafic BT by fractional crystallization from mafic tonalitic magma, an interpretation which is supported by common cumulitic texture in such rocks and by geochemical modelling by Lombardo *et al.* (2020). BT tonalites with tabular biotite and devoid of cumulitic texture can instead represent the result of direct emplacement at shallower levels of less mafic tonalite.

6.c. BT-PMBG

In the central sector of the promontory, weakly to unfoliated biotite tonalites are in contact, to the north and to the south, with the overlying PMBG unit. The granitoids from the top of the BT unit are mostly rather felsic tonalites with some samples also having leucotonalitic compositions representing crystallization from a residual tonalitic magma (Lombardo *et al.*, 2020). In the southern sector, the contact is marked by faults, as also highlighted by extreme rock fracturing and alteration, as well as by local slickenlines. On the other hand, in the northern sector, rare field evidence of sharp magmatic contacts between the two units is very well exposed (Fig. 8c). In more detail, at the roof of the tonalitic unit, emplacement of the overlying porphyritic granodioritic magma involved displacement of the tonalite, with local disaggregation in rounded blocks up to 1.5 meter in size (Fig. 8d). Such latter evidence indicates a rigid behaviour of the tonalites at the time of granodiorite emplacement, even though rare occurrence of hybrid rocks in the contact zone testifies for possible mixing processes also between the granodioritic magma and the mushy tonalite. Local shear bands, developed at the contact between MBPG and BT, are oriented in accordance with the magmatic fabric of the megacrystic granitoids (Fig. 8e). Finally, outstanding field evidence of the physical behaviour of mush systems is given by mechanical accumulation of K-feldspar megacrysts at places where the granodioritic magma was intruding the mushy tonalite, but only the liquid part of the magma was able to pass through, depicting a filter-press mechanism (Weinberg *et al.*, 2021 and references therein; Fiannacca *et al.*, 2024) (Fig. 8d).

7. Deformation microstructures

In the following paragraphs, we present the progressive deformation-induced microstructural evolution from supra- to sub-solidus high temperature (ca. 650°C > T > ca. 450°C) and, finally, low-temperature conditions (T < ca. 450°C) of the compositionally different CVP granitoids, in accordance with the guidelines proposed by Paterson *et al.* (1989), Bouchez *et al.* (1992), Stipp *et al.* (2002), Vernon (2000, 2018), Passchier & Trouw, (2005) and Law (2014).

7.a. Deformation microstructures in ABT

In general, the amphibole-biotite tonalites and quartz diorites show a strong to moderate planar fabric defined by preferential orientation of plagioclase, biotite and amphibole.

The magmatic texture is seldom preserved within low-strain domains and is characterized by euhedral to subhedral plagioclase and mostly subhedral biotite and amphibole.

Plagioclase is commonly affected by submagmatic microfractures, predominantly filled with quartz and occasionally also epidote, indicating deformation in the presence of melt at temperature conditions above ca. 700°C (Bouchez *et al.*, 1992; Fig. 9a and 9b). Local occurrence of irregular and lobate boundaries, preferentially observed at the contact with other plagioclase grains, reflects grain boundary migration (GBM) recrystallization, which also indicates deformation at suprasolidus conditions. More frequent, on the other hand, are the examples of submillimetric bulges at the crystal boundaries, as evidence of dominating bulging (BLG) recrystallization mechanism occurring at ca. 450°–600°C (Passchier & Trouw, 2005). Possible evidence for non-coaxial deformation comes from roundish and bent plagioclase crystals wrapped by biotite aggregates, appearing as porphyroclasts.

Deformation below ca. 500°C (Passchier & Trouw, 2005) is documented by widespread examples of deformed polysynthetic twins and kinked grains (Fig. 9b).

Quartz commonly shows chessboard extinction as a result of combined activation of basal and prism slip systems at submagmatic conditions (Fig. 9c). Elongated aggregates, produced by strong grain size reduction and surrounding large biotite fishes, are indicative of HT subsolidus deformation (Fig. 9d). Grains with extremely lobate boundaries as a result of grain boundary migration (GBM) recrystallization indicate deformation above ca. 500°C (Passchier & Trouw, 2005; Law, 2014; Fig. 9c and 9e). Core-and-mantle structures are rarely found (Fig. 9f). Subgrain rotation (SGR) recrystallization (Fig. 9f) and BLG recrystallization (Fig. 9e and 9f) largely occur, providing indications of continuous deformation down to the LT subsolidus regime, at T < ca. 400°C (Passchier & Trouw, 2005). Finally, undulose extinction, as well as deformation bands, is very frequent.

Biotite occurs in foliated aggregates wrapping large plagioclase grains with a dominant brittle behaviour, providing evidence of low- to medium- to high-temperature subsolidus deformation. Fish-like crystals provide further evidence of non-coaxial deformation (Fig. 9d). Solid-state deformation at medium temperature conditions is represented by dynamic recrystallization to smaller new grains (Fig. 9d). Intracrystalline plastic deformation of biotite is also highlighted by widespread examples of kink bands, which can develop in a wide range of temperatures, starting from ca. 250°C (Passchier & Trouw, 2005), thus not providing strong constraints.

Amphibole commonly shows evidence of brittle deformation (Fig. 9d) that indicates deformation below ca. 730°C (Passchier & Trouw, 2005). No evidence of plastic behaviour or recrystallization at suprasolidus conditions has been found for this phase.

7.b. Deformation microstructures in BT

Biotite tonalites and minor quartz diorites can display either a strong to moderate fabric (BT$_s$), or a weak to absent fabric (BT$_w$). BT$_s$ share with ABT the same strongly foliated structure and very similar deformation microstructures, developed at supra- to subsolidus low-temperature conditions. BT$_w$, on the other hand, despite exhibiting evidence of weak deformation, shows a more preserved magmatic texture. Magmatic microstructures are represented by sub-parallel alignment of euhedral and subhedral plagioclase crystals with regular polysynthetic twinning, subhedral-anhedral biotite plates and anhedral quartz.

Plagioclase is affected by quartz-filled microfractures indicating deformation at submagmatic conditions (T > ca. 700°C,
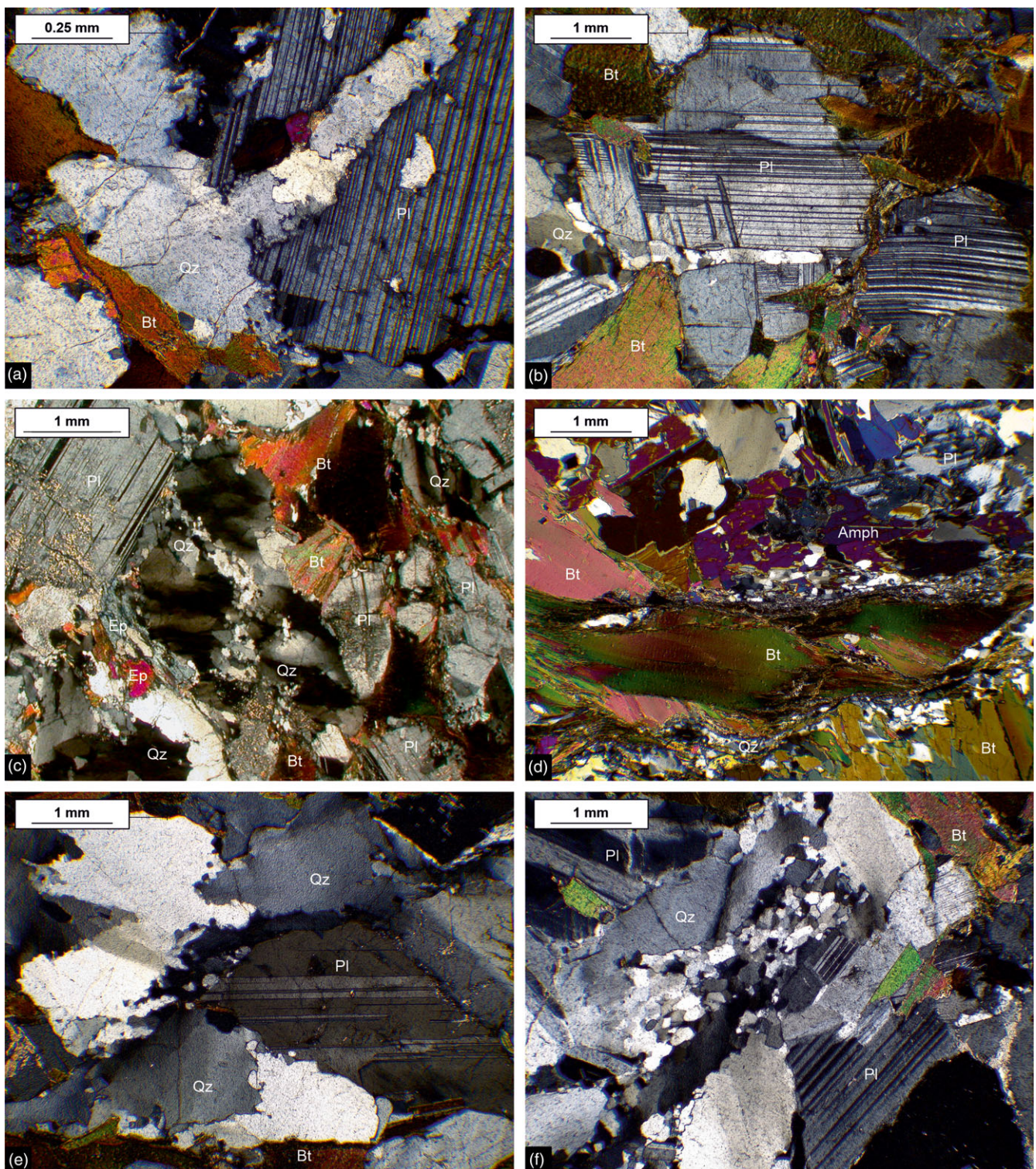
Figure 9. Deformation microstructures from suprasolidus to LT solid-state conditions in the amphibole-biotite tonalites and quartz diorites. (a) Submagmatic microfracture in plagioclase filled by quartz showing evidence of both high and low-temperature recrystallization (38°40′29″ N, 16°30′50″ E). (b) Plagioclase crystals surrounded by bent fish-like biotite individuals indicate high-temperature deformation. A submagmatic fracture filled by quartz, later affected by dynamic recrystallization, is also visible (38°43′36″ N, 16°02′21″ E). (c) Protomylonitic domain with quartz and plagioclase characterized by dynamic recrystallization along their borders. Quartz grains exhibit chessboard extinction overprinted by undulose extinction (38°36′23″ N, 15°51′01″ E). (d) High strain microdomain characterized by biotite fishes bordered by new grains of biotite and quartz dynamically recrystallized at HT subsolidus conditions (38°35′29″ N, 15°53′02″ E). (e) Strongly lobed edges in quartz represent examples of high-temperature recrystallization; smaller bulges at quartz boundaries are indicative of lower-temperature BLG recrystallization (38°36′23″ N, 15°52′24″ E). (f) SGR and BLG recrystallization of quartz crystals with undulose extinction (38°32′11″ N, 15°58′53″ E).
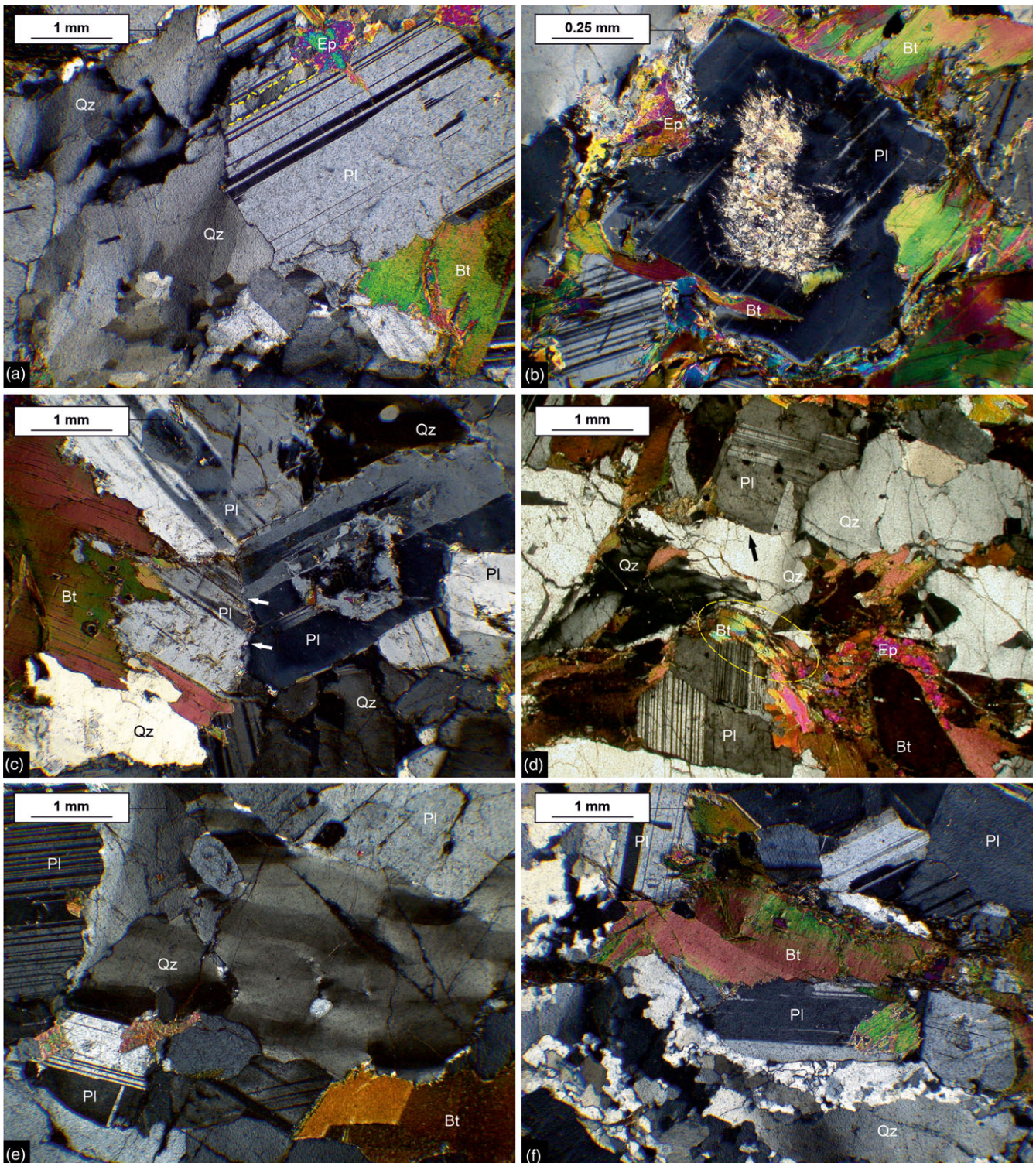
Figure 10. Deformation microstructures from submagmatic to solid-state domain in biotite tonalites and minor quartz diorites. (a) Thin submagmatic microfracture in a subhedral plagioclase surrounded by a deformed quartz aggregate showing recrystallised boundaries (38°34′48″ N, 15°54′37″ E). (b) Plastically deformed plagioclase with altered core bordered by stretched and fish-like biotite aggregates at its lower portion (38°41′18″ N, 15°59′56″ E). (c) Plagioclase crystals in a polygonal microdomain showing lobate boundaries (highlighted by white arrows), as result of grain boundary migration recrystallization (GBM) recrystallization (38°37′14″ N, 15°49′51″ E); (d) High strain zone highlighted by the presence of tiny biotite fishes (within the dashed yellow ellipse), deformed epidote crystals and quartz individuals with chessboard extinction. Bulging recrystallization at the boundary of a plagioclase crystals is indicated by the arrow (38°42′16″ N, 15°58′20″ E). (e) Undulose extinction in chessboard quartz with lobed edges indicating low-temperature deformation superimposing on submagmatic deformation (38°42′44″ N, 15°58′40″ E). (f) GBM recrystallization of quartz aggregates indicating deformation above ca. 500°C and widespread SGR developed at subsequent lower temperature (38°43′36″ N, 16°01′17″ E).

Bouchez *et al.*, 1992; Fig. 10a), common in the BT$_s$ and local in BT$_w$. Rounded grains wrapped by biotite, indicating non-coaxial deformation at HT subsolidus conditions are often found, more commonly in the BT$_s$ (Fig. 10b). GBM recrystallization occurs in plagioclase from the BT$_s$ while no evidence has been detected in BT$_w$ (Fig. 10c). BLG recrystallization is frequently recorded in crystals from both BT$_s$ and BT$_w$ and indicates deformation below ca. 600°C (Passchier & Trouw, 2005; Fig. 10d). Low-temperature deformation is evidenced by many examples of kink bands in euhedral crystals as well as by the occurrence of deformation twins or flame-shape twinning.

Quartz exhibits diffuse chessboard extinction representing evidence of deformation at submagmatic conditions (Fig. 10e). Extremely lobate boundaries at the contact with both plagioclase and other quartz crystals indicate GBM recrystallization, at HT subsolidus conditions (Fig. 10a, 10c and 10e). Fine-grained elongated aggregates with undulose extinction occur locally in BT$_s$ along deformed microdomains. Examples of solid-state lower temperature deformation come from subgrain rotation (SGR) recrystallization, represented by oriented polycrystalline aggregates (Fig. 10f). Very small bulges along the crystal boundaries, superimposing also on the new grains formed at higher temperature, testify ongoing deformation at temperature below ca. 400°C (Passchier & Trouw, 2005; Law, 2014).

Biotite commonly occurs in strongly elongated aggregates bordering larger plagioclase crystals in BT$_s$ (Fig. 10b, 10d and 10f). In the same rocks, and more locally in the BT$_w$, biotite often occurs as mica fish, suggestive of non-coaxial deformation (Fig. 10d). Deformation at low-temperature subsolidus conditions is also represented by widespread evidence of kink bands. Along highly deformed zones, submillimetric new grains nucleate at the boundaries of deformed crystals, as indication of solid-state deformation.

7.c. Deformation microstructures in PMBG

Porphyritic two-mica granitoids are weakly to mainly undeformed rocks, with a sporadic fabric mainly defined in the field by the preferred orientation of K-feldspar megacrysts while being mainly highlighted in thin section by iso-oriented fine-grained biotite-muscovite trails. Unlike the tonalites, the magmatic structure is typically well preserved and only slightly and locally reworked by deformation. The matrix consists of subhedral weakly zoned plagioclase usually with regular polysynthetic twinning, subhedral perthitic microcline and biotite plates often intergrown or surrounded by muscovite and anhedral quartz.

Plagioclase rarely shows quartz-filled microfractures providing evidence of deformation at submagmatic conditions (Fig. 11a). Asymmetric pressure shadows bordering rounded plagioclase grains in high strain zones are consistent with non-coaxial HT subsolidus deformation (Passchier & Trouw, 2005; Fig. 11b). Myrmekitic intergrowths, in contact with K-feldspar crystals, may indicate deformation temperatures from ca. 450°C (Passchier & Trouw, 2005). Frequently, BLG recrystallization, suggesting deformation below 600°C (Passchier & Trouw, 2005), affects the boundaries of the grains in contact with other plagioclase crystals. Subsolidus lower temperature deformation twins occur widely. Rare kink bands are also observed.

Microcline commonly contains flame perthites, as a result of albite exsolution in K-feldspar that has undergone solid-state deformation (Pryer and Robin, 1995, 1996; Vernon, 2018),

particularly found in large K-feldspar crystals, while being less common in smaller ones (Fig. 11c). Bent albite-pericline twinning, as well as BLG recrystallization along the boundaries, is locally found (Fig. 11c).

Quartz usually exhibits chessboard extinction pattern, documenting deformation at submagmatic conditions (T > 650°C, Passchier & Trouw, 2005; Law, 2014), partially masked by widespread dominant undulose extinction (Fig. 11d). High-temperature subsolidus GBM recrystallization is common along crystals boundaries (Fig. 11e), while evidence of lower temperature SGR recrystallization, localized in fine-grained microdomains, is less common. BLG recrystallization, indicating deformation below 400°C (Passchier & Trouw, 2005; Law, 2014), is widespread and develops at the contact with feldspar and, especially, quartz (Fig. 11f).

Biotite is locally elongated in a mica-fish geometry, suggesting non-coaxial deformation above ca. 250°C (Passchier & Trouw, 2005). Kink bands frequently occur.

Muscovite shows deformation similar to biotite (Fig. 11b and f).

8. Discussion

8.a. Geology and structure of Capo Vaticano Promontory

Field observations coupled with microscopic investigations allowed the recognition of three compositionally and structurally different plutonic units in the Capo Vaticano Promontory. A discontinuous MBZ made of garnet-bearing migmatitic paragneisses and strongly to weakly foliated quartz-diorites and tonalites marks the passage from the lower-crustal metamorphic rocks to the deepest emplaced granitoids.

Primary contacts between the different magmatic units are rarely exposed in the whole study area. The transitional contact between the floor of the batholith and the high-grade metamorphic basement, observed in the MBZ, is characterized by widespread evidence of extensive crustal melting, triggered by the intrusion of the granitoid body in the already anatectic basement at an estimated depth of ca. 21 km (Caggianelli *et al.*, 1997). The main evidence of this interaction is represented by large volumes of anatectic melts interacting by mixing/mingling processes with the cooling tonalitic-quartz dioritic magma; the process is highlighted by the presence in the ABT of large peritectic garnet crystals produced by Bt-dehydration melting of the host paragneisses as a consequence of the heat released by the crystallizing magma (Clarke & Rottura, 1994; Fiannacca *et al.*, 2024). Relationships between ABT and BT were not directly observed but, based on our field and thin-section investigations, ABT occurs at the deepest batholith levels, transitioning upward to BT$_s$ and then to BT$_w$, the latter therefore representing the top of the tonalitic unit of the Serre Batholith in the CVP area. This is also observed in the Serre Massif where, nevertheless, both ABT and BT$_s$ are in direct contact with the MBZ at the batholith floor (Russo *et al.*, 2023). In both CVP and Serre Massif, a link by fractional crystallization between ABT and BT is supported by petrographic and geochemical evidence (Lombardo *et al.*, 2020; Russo *et al.*, 2023). Sharp magmatic contacts have been observed between BT$_w$ and overlying PMBG, with clear evidence of the granodioritic magma intruding and locally dismembering the tonalites when the latter were mostly solidified.

Amphibole-biotite tonalites and biotite tonalites constitute, together with minor quartz-diorites, the majority of the exposed outcrops and occupy the most peripheral sectors of the study area.
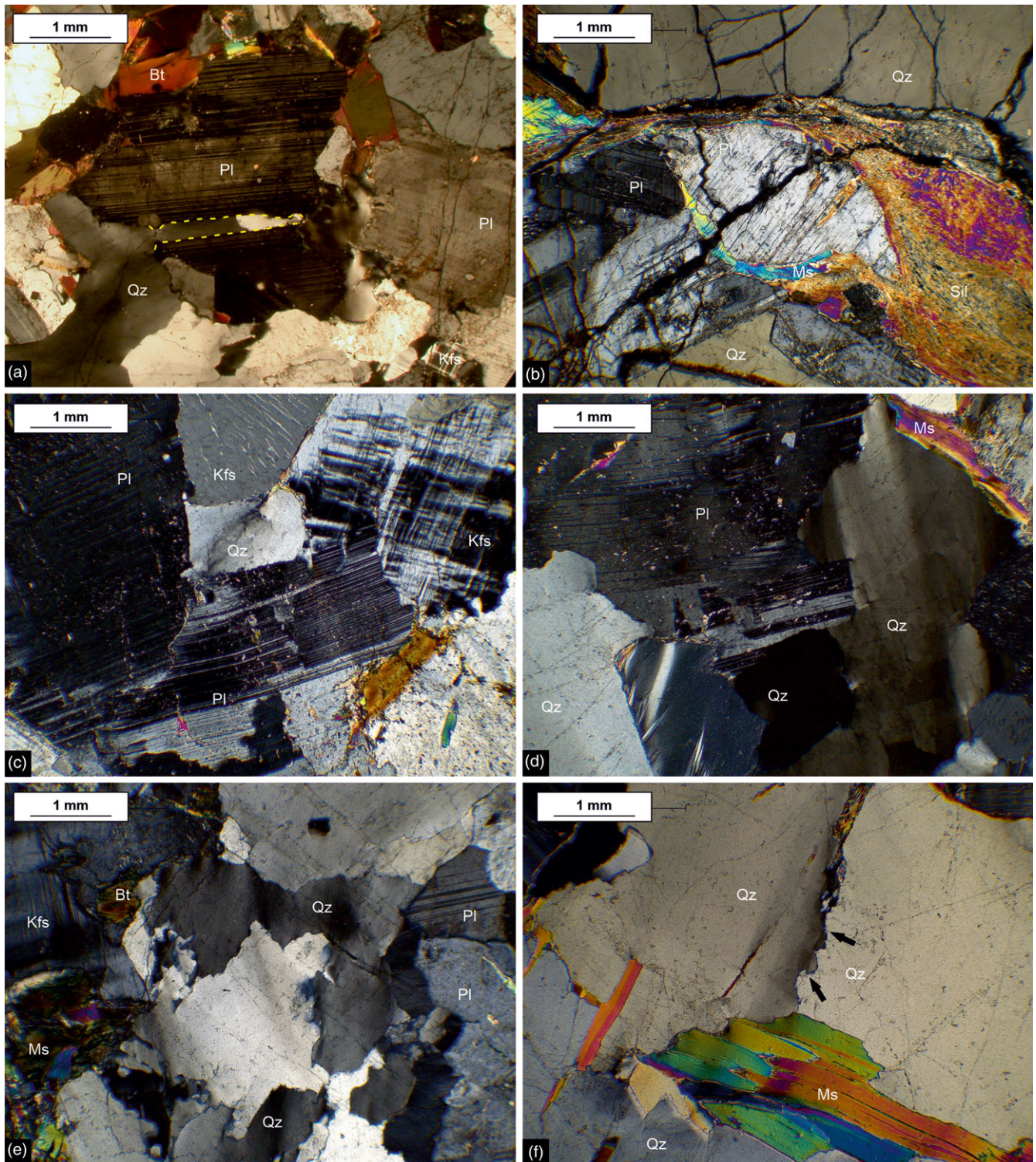
Figure 11. Deformation microstructures from submagmatic to solid-state domain in muscovite-biotite porphyritic granodiorites and granites. (a) Deformation at submagmatic condition is marked by local occurrence of quartz-filled microfractures in plagioclase crystals (38°38′28″ N, 15°55′09″ E). (b) Incipient σ-type plagioclase porphyroclast with anastomosing muscovite/sillimanite folia is indicative of deformation at high-temperature conditions (38°38′35″ N, 15°53′35″ E). (c) Deformation below 450°C is indicated by kinked subhedral plagioclase crystal, deformed cross-hatched twinning in microcline and flame perthites (38°38′48″ N, 15°50′28″ E). (d) Quartz grain showing a chessboard extinction pattern indicative of deformation temperature above 650°C (38°41′05″ N, 15°55′13″ E). (e) Very lobate edges in quartz grains representing evidence of grain boundary migration recrystallization recrystallization (38°41′11″ N, 15°56′49″ E). (f) Bulging recrystallization along wavy edges of quartz grains represent, together with kinked muscovite sheets, examples of deformation at low-temperature conditions (38°40′50″ N, 15°55′39″ E).

The central sector, on the other hand, is characterized by porphyritic muscovite-biotite granodiorites and granites, which pass to the underlying BT in the northern sector with a sharp magmatic contact, while in the southern sector, the two units come into contact through fault zones.

In addition, our field results reveal that the CVP is subdivided into two sectors by an inferred WNW-ESE tectonic lineament, roughly running along the Fiumara di Brattirò, from Torre Ruffa on the Tyrrhenian coast to, at least, north-east of Spilinga in the inland (Fig. 3). We name here this tectonic lineament Brattirò Fault. This new perspective is based on the occurrence, to the north of the fault, of a continuous exposure of the granitoids that make up the deep-intermediate levels of Serre Batholith, together with their lower-crustal migmatitic host rocks (Fig. 3). On the other hand, the CVP sector south of the fault is made up only of the lowermost batholith levels and MBZ, with a more chaotic arrangement, as a result of several recent faults that exerted in this sector a stronger control on the exposure and distribution of the outcrops (Fig. 3).

Fabric intensity shows a direct relationship with emplacement depth of the Capo Vaticano granitoids. In particular, fabric ranges from strong to moderate in the ABT and BT_s rocks from the lowermost levels, from mostly weak to locally absent in the overlying BT_w, and, finally, from locally weak to mainly absent in the PMBG, which represents the youngest and shallowest granitoids in the CVP. Among the ABT and BT, the strongest fabric is recorded in the Joppolo and Zambrone area, to the southwest and northeast of the promontory, respectively; in contrast, the weakest fabric is found in the central sector. No clear correlation between fabric intensity and geographical distribution of the outcrops can be defined in the southern CVP (south of Fiumara di Brattirò; Fig. 3), where post-Variscan tectonics caused a strong reworking of the original structural setting within and between the exposed magmatic units.

8.b. Emplacement and supra- to sub-solidus deformation of the Capo Vaticano granitoids

Granitoids from Capo Vaticano Promontory exhibit a wide variety of deformation microstructures developed during cooling from suprasolidus to progressively lower temperature subsolidus conditions, where the latter typically tend to obliterate the previous ones (Figs. 9–11).

It can be therefore reasonable to assume that also the fabric observed in the granitoids started to develop at supra-solidus conditions.

Clear examples of supra-solidus deformation are represented by quartz chessboard patterns partially obliterated by a dominant undulose extinction, or by evidence of low-T recrystallization of quartz filling submagmatic microfractures in feldspars.

The supra- to subsolidus evolution of the different granitoid rocks is illustrated in a microstructural scheme (Fig. 12) aimed to summarize and compare the deformation experienced during cooling of the magmatic bodies, as recorded by the different mineral phases in each magmatic unit.

Deformation microstructures developed at suprasolidus to LT subsolidus conditions have been observed both within the same thin section and across different thin sections throughout the whole study area; they occur with very similar frequency in both ABT and BT_s. In contrast, BT_w rocks, from the top of the BT unit, exhibit a degree and type of deformation more similar to that of the overlying PMBG.

Submagmatic microstructures, such as chessboard extinction in quartz and less common GBM and SGR recrystallization in plagioclase, are quite equally distributed in the ABT and BT. Quartz chessboard patterns are also present in PMBG, while no evidence of high-temperature recrystallization of feldspar has been found in the latter rocks (and BT_w). This might be due to both the decreasing intensity of deformation during the emplacement of the megacrystic granodiorites-granites, consistent with the much stronger fabric in the older and deeper tonalites, and to the emplacement temperature of the PMBG, lower than that required to develop GBM in feldspars (ca. 850°C). This interpretation might also hold for the BT_w, which is a more felsic tonalite emplaced at the top of the BT unit, because of their shorter residence time at high-temperature conditions; the latter is again a combined consequence of emplacement at relatively shallower depth and lower emplacement temperature compared to the deeper and more mafic tonalites-quartz diorite. Similar interpretations were already given by Caggianelli *et al.* (2000a) to explain the stronger HT deformation recorded in the tonalites from the Serre Massif compared to the upper crustal Bt±Am granodiorites; the same authors did not investigate the PMBG. Submagmatic microfractures in plagioclase are more preserved in the deep ABT unit and they are gradually less common towards the shallower PMBG. Occurrence of submagmatic fractures and chessboard patterns in all three magmatic units suggests that all of them were affected by deformation at supra-solidus conditions, with the strongest fabric developed in the ABT from the deepest levels of the batholith.

Most of the high-temperature subsolidus deformation microstructures have a different distribution in the three granitoid units. High-temperature dynamic recrystallizations, such as feldspar bulging, GBM recrystallization in quartz and dynamic recrystallization in mica, occur with higher frequency in the ABT, consistently with the higher residence time at high temperature of such rocks. Myrmekites and flame perthites are frequently observed in K-feldspar crystals exclusively from PMBG, which are the only rock types containing this mineral. Mica kinking and mica fish are observed in all three units, with a distribution directly related to the emplacement depth of the studied granitoid units.

The most commonly observed structural features, in all the magmatic units, are subsolidus low-temperature deformation microstructures. Among these, kink bands in mica, quartz and feldspar as well as plagioclase porphyroclasts, and SGR recrystallization in quartz are gradually more abundant towards the deepest ABT, while deformation twins in plagioclase together with undulose extinction and BLG recrystallization in quartz occur with similar frequency in all the three magmatic units. This difference leads us to consider the first group of low-T deformation microstructures as more diagnostic in the study of the relationships between tectonics and emplacement-cooling of granitoid magmas in composite batholiths.

On the other hand, low-temperature subsolidus microstructures largely overprinting those developed under submagmatic and high-temperature subsolidus conditions, indicate continuous deformation during cooling of the granitoid magmas.

Figure 13 provides a geospatial view of the obtained microstructural data by means of semi-quantitative maps of the different types of microstructures recorded in the studied samples, across the whole CVP. Based on the extent of deformation observed in thin section, deformation microstructures occupy approximately 40% to 70% of the area in each investigated thin section. The contour maps (Fig. 13a–d) indicate regions that experienced more
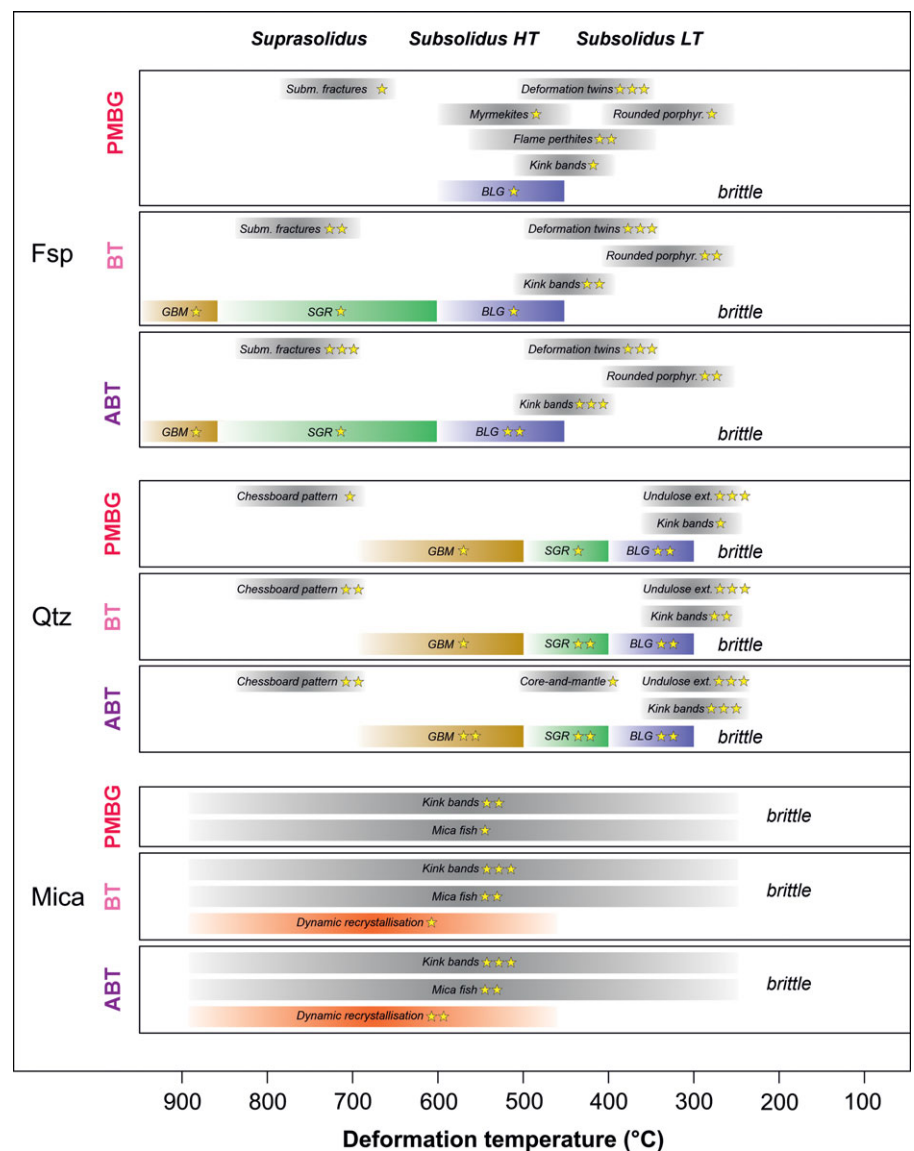
Figure 12. Microstructural scheme of the deformation recorded by various minerals (feldspar, quartz, and mica) in the studied granitoid rocks and corresponding thermal ranges, from submagmatic to low-T solid state. Temperature range estimates after Passchier & Trouw (2005) and Vernon, 2018). BLG = bulging recrystallization; SGR = subgrain rotation recrystallization; GBM = grain boundary migration recrystallization; subm. = submagmatic; porphyr. = porphyroclast; ext. = extinction. Single, double and triple star indicate rare, common and very common occurrence, respectively.

intense or specific types of deformation, with the PMBG from the central part of the whole study area representing the least deformed granitoids.

Submagmatic and HT subsolidus microstructures (Fig. 13b and 13c) are, in general, the least abundant microstructures and occur with higher frequency in the deeper granitoids in both the northern and southern CVP outcrops. LT subsolidus microstructures (Fig. 13d) are instead the main deformation-related features in all the studied granitoids, as they represent the last recorded deformation evidence, largely obliterating the higher temperature ones.

Notably, the maps confirm our field hypothesis of a continuous section from the deep to the intermediate levels of the Serre Batholith in the northern area. In particular, Fig. 13a reveals a decreasing strain gradient from the northern region to the central area with the granitoids gradually less deformed towards southwest, where the shallowest and youngest PMBG crop out, in accordance with the proposed existence of a continuous crustal section in that region. Additionally, the contour lines align with the geometry of the contacts in the same sector. In contrast, in the southern CVP sector, there is no clear relationship between location and type of preserved deformation microstructures, nor the contour lines are in accordance with the magmatic contacts (Fig. 3) as result of the recent fault systems activity, more pervasive in this sector.

All the above microstructural evidence implies that tectonic stress was active during the cooling history of the magmatic units, starting from suprasolidus conditions up to the latest evidence of deformation at low-temperature conditions, below 450°C. Furthermore, in the deepest levels of the ABT-BT units, a strong foliation is always recognizable in the field, while planar fabric is faint and sometimes absent in the shallower levels. Despite magmatic foliations can develop during ascent and emplacement of granitoid magmas also in absence of tectonic stress, the continuum between suprasolidus and high-temperature solid-state deformation processes during the development of the main foliation strongly suggests a syn-tectonic emplacement for the deep-emplaced granitoids (Paterson *et al.*, 1989; Vernon, 2000, 2018). A tectonically-controlled magma emplacement has been already suggested for the same deep crustal granitoids in the Serre
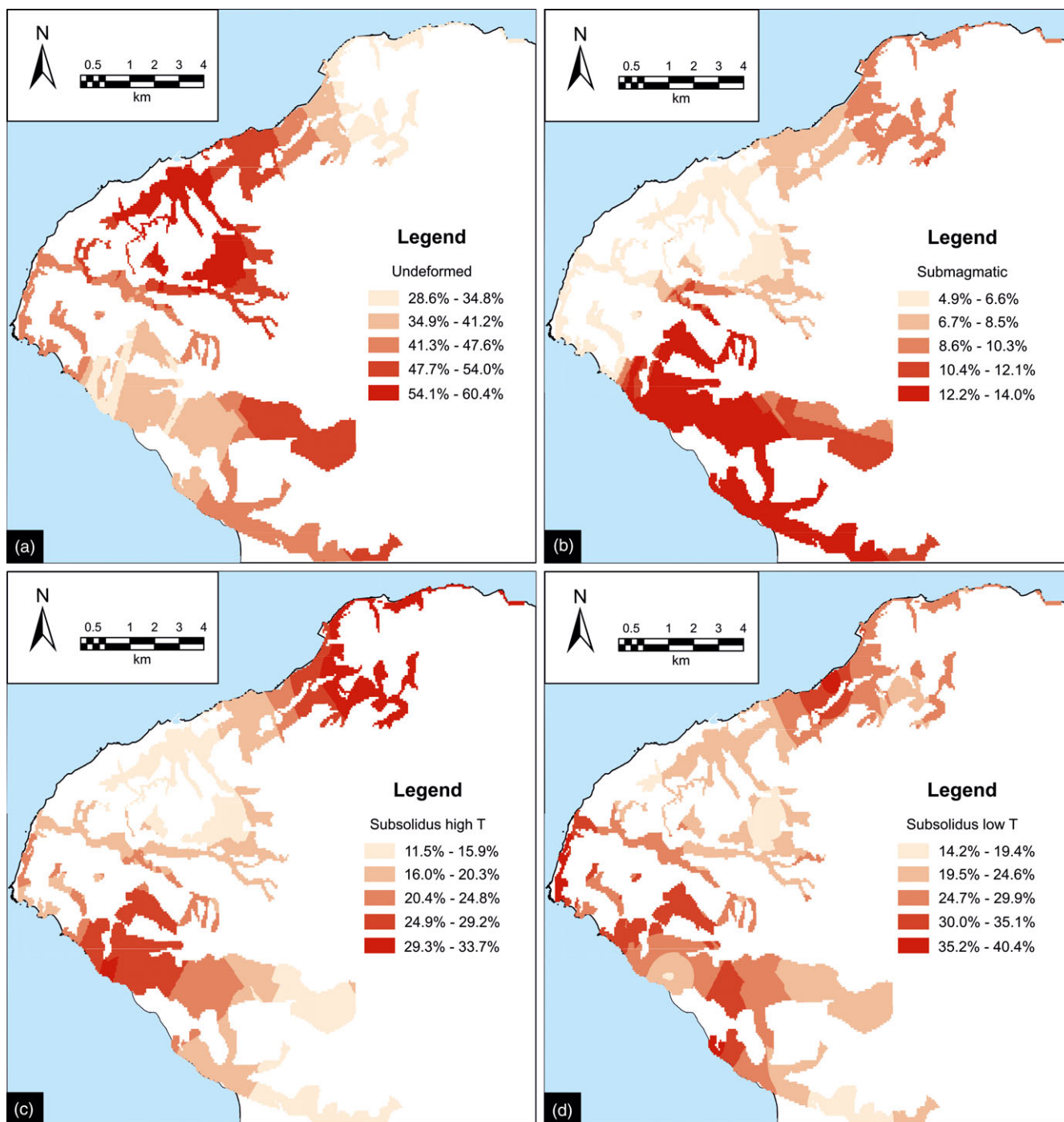
Figure 13. Spatial interpolation of the semi-quantitative analysis of the magmatic (a), submagmatic (b), subsolidus HT (c) and subsolidus HT (d) microstructures across the whole Capo Vaticano Promontory. The interpolation maps were obtained by applying the Empirical Bayesian Kriging tool to the available microstructural data in the ArcGIS® environment. The method applied was "Equal Interval", giving an equal interval distribution in the selected classes, with the data range of each class held constant. Data were divided into five classes, resulting to provide the most informative outputs. The percentages in the legend represent the amount of the thin section area which is undeformed (Figure 13a) or recording deformation developed at submagmatic or subsolidus high temperature to low-temperature conditions (Figures 13b, 13c and 13d, respectively).

Batholith (Rottura *et al.*, 1990; Caggianelli *et al.*, 2000b; Russo *et al.*, 2023). Since no well-developed fabric is present in the PMBG unit, a strong correlation between tectonics and fabric cannot be clearly established for these deep-intermediate granitoids. Nevertheless, continuous supra- to LT subsolidus deformation during granitoid cooling has been identified in thin section, also for the shallower CPV granitoids. This would suggest that the shallower and younger PMBG also emplaced syntectonically, but during waning stages of late Variscan post-collisional tectonics.

9. Conclusions

This study has shed new light on the batholith architecture and on the possible relationships between tectonics and post-collisional

granitoid magmatism at Capo Vaticano Promontory, a dislocated portion of the late Variscan Serre Batholith, through field and microstructural investigations.

A detailed field survey allowed us to realize the first detailed geological map of the outcropping magmatic units, at a scale of 1:140,000, as well as to define the relationships between the plutonic units. This allowed to separate the CVP into two sectors, a northern sector exposing a continuous cross-section of the batholith, from the deepest tonalites/quartz diorites to intermediate-seated porphyritic two-mica granitoids, and a southern sector only exposing the deepest levels, but with no regular arrangement due to strong post-Variscan tectonic disturbance.

A MBZ represents the transition between the metamorphic basement, mainly constituted by migmatitic paragneisses, and strongly to moderately foliated quartz diorites and tonalites (ABT and overlying BT_s), which make up the lowermost levels of the exposed magmatic complex. The strongly to moderately foliated ABT-BT_s pass upward to weakly foliated to nearly isotropic tonalites (BT_w). The latter are overlain by means of sharp magmatic contacts, by porphyritic two-mica granodiorites and granites (PMBG), only locally foliated, which represent the intermediate levels of the Serre Batholith and the top of the exposed magmatic complex in the Capo Vaticano Promontory.

Microstructural investigations highlighted a wide range of deformation microstructures that indicate, for the strongly to moderately foliated rocks, a tectonic stress operating already at suprasolidus conditions, and continuing at progressively decreasing temperatures up to low-temperature subsolidus conditions (T < 450°C). A clear field fabric is rarely present in the weakly to non-foliated BT_w and PMBG; for these latter rocks, we can only confidently state that at submagmatic conditions (T > 650°C), stress was already ongoing down to, progressively, low-temperature sub-solidus conditions (T < 450°C). A direct correlation between intensity of recorded deformation and emplacement depth and age, as well as composition, of the studied lithotypes was found in the northern CVP sector.

Continuous supra- to subsolidus deformation associated with development of the main foliation appears consistent with a syntectonic emplacement for the early and deep ABT and BT; in particular, field and microstructural evidence of deformation would suggest tectonically-controlled magma emplacement, as already proposed for the same deep crustal granitoids in the Serre Batholith.

Similar, though much less intense, deformation recorded in the shallower and younger PMBG suggests a similar emplacement scenario for the PMBG magma, yet during waning stages of tectonic activity associated with the post-collisional evolution of the Variscan Belt in south-western Europe.

References

Angì G, Cirrincione R, Fazio E, Fiannacca P, Ortolano G and Pezzino A (2010) Metamorphic evolution of preserved Hercynian crustal section in the Serre Massif (Calabria–Peloritani Orogen, southern Italy). *Lithos* **115**, 237–262.

Behr HJ, Engel W, Franke W, Giese P and Weber K (1984) The Variscan belt in Central Europe: main structures, geodynamic implications, open questions. *Tectonophysics* **109**, 15–40.

Bianca M, Catalano S, De Guidi G, Gueli AM, Monaco C, Ristuccia GM, Stella G, Tortorici G and Troja SO (2011) Luminescence chronology of Pleistocene marine terraces of Capo Vaticano peninsula (Calabria, southern Italy). *Quaternary International* **232**, 114–121.

Bouchez JL, Delas C, Gleizes G, Nédélec A and Cuney M (1992) Submagmatic microfractures in granites. *Geology* **20**, 35–38.

Bouchez JL and Diot H (1990) Nested granites in question: Contrasted emplacement kinematics of independent magmas in the Zaër pluton, Morocco. *Geology* **18**, 966–969.

Brown M (2013). Granite: From genesis to emplacement. *GSA bulletin* **125**, 1079–1113.

Brown M and Solar GS (1999) The mechanism of ascent and emplacement of granite magma during transpression: a syntectonic granite paradigm. *Tectonophysics* **312**, 1–33.

Burg JP, Bale P, Brun JP and Girardeau J (1987) Stretching lineation and transport direction in the Ibero-Armorican arc during the Siluro-Devonian collision. *Geodinamica Acta* **1**, 71–87.

Burton AN (1971) Carta geologica della Calabria alla scala 1:25.000: relazione generale. Ufficio bonifiche. Ufficio piani di massima e studi.

Caggianelli A, Del Moro A, Paglionico A, Piccarreta G, Pinarelli L and Rottura A (1991) Lower crustal granite genesis connected with chemical fractionation in the continental crust of Calabria (Southern Italy). *Eur. J. Mineral* **3**, 159–180.

Caggianelli A, Liotta D, Prosser G and Ranalli G (2007) Pressure–temperature evolution of the late Hercynian Calabria continental crust: compatibility with post-collisional extensional tectonics. *Terra Nova* **19**, 502–514.

Caggianelli A, Prosser G and Del Moro A (2000b) Cooling and exhumation history of deep-seated and shallow level, late Hercynian granitoids from Calabria. *Geological Journal* **35**, 33–42.

Caggianelli A, Prosser G and Di Battista P (1997) Textural features and strain of granitoids emplaced at different depths: the example of the Hercynian tonalites and granodiorites from Calabria. *Mineralogica et Petrographica Acta* **40**, 11–26.

Caggianelli A, Prosser G, Festa V, Langone A and Spiess R (2013) From the upper to the lower continental crust exposed in Calabria. *Geological Field Trips and Maps* **5**, 1–49.

Caggianelli A, Prosser G, Rottura A (2000a) Thermal history vs. fabric anisotropy in granitoids emplaced at different crustal levels: an example from Calabria, southern Italy. *Terra Nova* **12**, 109–116.

Carosi R, Petroccia A, Iaccarino S, Simonetti M, Langone A and Montomoli C (2020) Kinematics and timing constraints in a transpressive tectonic regime: the example of the Posada-Asinara Shear Zone (NE Sardinia, Italy). *Geosciences* **10**, 288.

Cirrincione R, Fazio E, Fiannacca P, Ortolano G, Pezzino A and Punturo R (2015) The Calabria-Peloritani Orogen, a composite terrane in Central Mediterranean; its overall architecture and geodynamic significance for a pre-Alpine scenario around the Tethyan basin. *Periodico di Mineralogia* **84**, 701–749.

Clarke DB and Rottura A (1994) Garnet-forming and garnet-eliminating reactions in a quartz diorite intrusion at Capo Vaticano, Calabria, Italy. *The Canadian Mineralogist* **32**, 623–35.

Colonna V, Lorenzoni S and Zanettin Lorenzoni E (1973) Sull'esistenza di due complessi metamorfici lungo il bordo sud-orientale del massiccio granitico delle Serre (Calabria). *Bollettino della Società Geologica Italiana* **92**, 801–830.

Conforti M and Ietto F (2020) Influence of tectonics and morphometric features on the landslide distribution: a case study from the Mesima Basin (Calabria, South Italy). *Journal of Earth Science* **31**, 393–409.

Corsini M and Rolland Y (2009) Late evolution of the southern European Variscan belt: Exhumation of the lower crust in a context of oblique convergence. *Comptes Rendus Geoscience* **341**, 214–223.

Cruden AR and Weinberg RF (2018) Mechanisms of magma transport and storage in the lower and middle crust—magma segregation, ascent and emplacement. In *Volcanic and Igneous Plumbing Systems* (ed S Burchardt), pp. 13–53. Amsterdam: Elsevier.

Demartis M, Pinotti LP, Coniglio JE, D'Eramo FJ, Tubía JM, Aragón E and Insúa LAA (2011) Ascent and emplacement of pegmatitic melts in a major reverse shear zone (Sierras de Córdoba, Argentina). *Journal of Structural Geology* **33**, 1334–1346.

Elter FM, Gaggero L, Mantovani F, Pandeli E and Costamagna LG (2020) The Atlas-East Variscan-Elbe shear system and its role in the formation of the pull-apart Late Palaeozoic basins. *International Journal of Earth Sciences* **109**, 739–760.

Fazio E, Fiannacca P, Russo D and Cirrincione R (2020) Submagmatic to solid-state deformation microstructures recorded in cooling granitoids during exhumation of late-Variscan crust in North-Eastern Sicily. *Geosciences* **10**, 311.

Festa V, Caggianelli A, Langone A and Prosser G (2013) Time–space relationships among structural and metamorphic aureoles related to granite emplacement: a case study from the Serre Massif (southern Italy). *Geological Magazine* **150**, 441–454.

Festa V, Fornelli A, Paglionico A, Pascazio A, Piccarreta G and Spiess R (2012) Asynchronous extension of the late-Hercynian crust in Calabria. *Tectonophysics* **518**, 29–43.

Fiannacca P, Cirrincione R, Bonanno F and Carciotto MM (2015) Source-inherited compositional diversity in granite batholiths: the geochemical message of Late Paleozoic intrusive magmatism in central Calabria (southern Italy). *Lithos* **236**, 123–140.

Fiannacca P, Russo D, Fazio E and Cirrincione R (2024) Calabria coast to coast: a nearly complete cross-section of continental crust with a 13 km-thick late Variscan batholith. *Geological Field Trips and Maps* **16**, 1–84.

Fiannacca P, Russo D, Fazio E, Cirrincione R and Mamtani MA (2021) Fabric analysis in upper crustal post-collisional granitoids from the Serre Batholith (Southern Italy): Results from microstructural and AMS investigations. *Geosciences* **11**, 414.

Fiannacca P, Williams IS and Cirrincione R (2017) Timescales and mechanisms of batholith construction: Constraints from zircon oxygen isotopes and geochronology of the late Variscan Serre Batholith (Calabria, southern Italy). *Lithos* **277**, 302–314.

Fornelli A, Caggianelli A, Del Moro A, Bargossi GM, Paglionico A, Piccarreta G and Rottura A (1994). Petrology and evolution of the Central Serre granitoids (southern Calabria–Italy). *Periodico di Mineralogia* **63**, 53–70.

Fornelli A, Pascazio A and Piccarreta G (2012) Diachronic and different metamorphic evolution in the fossil Variscan lower crust of Calabria. *International Journal of Earth Sciences* **101**, 1191–1207.

Fornelli A, Piccarreta G, Acquafredda P, Micheletti F and Paglionico A (2004) Geochemical fractionation in migmatitic rocks from Serre granulitic terrane (Calabria, southern Italy). *Periodico di Mineralogia* **73**, 145–57.

Fornelli A, Piccarreta G, Del Moro A and Acquafredda P (2002). Multi-stage melting in the lower crust of the Serre (Southern Italy). *Journal of Petrology* **43**, 2191–2217.

Ghisetti F and Vezzani L (1981) Contribution of structural analysis to understanding the geodynamic evolution of the Calabrian arc (Southern Italy). *Journal of Structural Geology* **3**, 371–381.

Law RD (2014) Deformation thermometry based on quartz c-axis fabrics and recrystallization microstructures: A review. *Journal of Structural Geology* **66**, 129–161.

Lombardo R (2020) Role of granitoid magmatism in the growth and evolution of the continental crust: a petrological and geochronological study of quartz-diorites and tonalites from a type section of late-paleozoic continental crust (Serre Batholith, southern Italy). PhD thesis, Dipartimento di Scienze Biologiche, Geologiche ed Ambientali, Università di Catania.

Lombardo R, Fiannacca P and Cirrincione R (2020) Geochemical modelling of granitoid magma diversity at Capo Vaticano Promontory (Serre Batholith, southern Italy). *Geochemistry* **80**, 125599.

Matte P (1986) Tectonics and plate tectonics model for the Variscan belt of Europe. *Tectonophysics* **126**, 329–374.

Monaco C and Tortorici L (2000) Active faulting in the Calabrian arc and eastern Sicily. *Journal of Geodynamics* **29**, 407–424.

Navas-Parejo P, Somma R, Rodríguez-Cañero R, Martín-Algarra A and Perrone V (2015) Conodont-based stratigraphy in the Devonian of the Serre Massif (southern Italy). *Stratigraphy* **12**, 1–21.

Ortolano G, Pagano M, Visalli R, Angì G, D'Agostino A, Muto F, Tripodi V, Critelli S and Cirrincione R (2022) Geology and structure of the Serre Massif upper crust: a look in to the late-Variscan strike–slip kinematics of the Southern European Variscan chain. *Journal of Maps* **18**, 314–330.

Padovano M, Dörr W, Elter F M and Gerdes A (2014) The east Variscan shear zone: Geochronological constraints from the Capo Ferro area (NE Sardinia, Italy). *Lithos* **196**, 27–41.

Padovano M, Elter F M, Pandeli E and Franceschelli M (2012) The East Variscan Shear Zone: new insights into its role in the Late Carboniferous collision in southern Europe. *International Geology Review* **54**, 957–970.

Passchier CW and Trouw RA (2005) *Microtectonics*. New York City: Springer Science & Business Media.

Paterson SR, Vernon RH and Tobisch OT (1989) A review of criteria for the identification of magmatic and tectonic foliations in granitoids. *Journal of Structural Geology* **11**, 349–363.

Perri F, Ietto F, Le Pera E and Apollaro C (2016) Weathering processes affecting granitoid profiles of Capo Vaticano (Calabria, southern Italy) based on petrographic, mineralogic and reaction path modelling approaches. *Geological Journal* **51**, 368–386.

Petford N and Clemens JD (2000) Granites are not diapiric! *Geology Today* **16**, 180–184.

Pryer LL and Robin PY (1995) Retrograde metamorphic reactions in deforming granites and the origin of flame perthite. *Journal of Metamorphic Geology* **13**, 645–658.

Pryer LL and Robin PY (1996) Differential stress control on the growth and orientation of flame perthite: a palaeostress-direction indicator. *Journal of Structural Geology* **18**, 1151-1166.

Romano V, Cirrincione R, Fiannacca P, Lustrino M and Tranchina A (2011) Late-Hercynian post-collisional dyke magmatism in central Calabria (Serre Massif, southern Italy). *Periodico di Mineralogia* **80**, 489–515.

Rottura A, Bargossi GM, Caironi V, Del Moro A, Maccarrone E, Macera P, Paglionico A, Petrini R, Piccareta G and Poli G (1990) Petrogenesis of contrasting Hercynian granitoids from the Calabrian Arc, southern Italy. *Lithos* **24**, 97–119.

Rottura A, Del Moro A, Pinarelli L, Petrini R, Peccerillo A, Caggianelli A, Bargossi GM and Piccarreta G (1991) Relationships between intermediate and acidic rocks in orogenic granitoid suites: petrological, geochemical and isotopic (Sr, Nd, Pb) data from Capo Vaticano (southern Calabria, Italy). *Chemical Geology* **92**, 153–176.

Russo D, Fiannacca P, Fazio E, Cirrincione R and Mamtani MA (2023) From floor to roof of a batholith: Geology and petrography of the north-eastern Serre Batholith (Calabria, southern Italy). *Journal of Maps* **19**, 2149358.

Schenk V (1980) U-Pb and Rb-Sr radiometric dates and their correlation with metamorphic events in the granulite-facies basement of the Serre, Southern Calabria (Italy). *Contributions to Mineralogy and Petrology* **73**, 23–38.

Schenk V (1981) Synchronous uplift of the lower crust of the Ivrea Zone and of southern Calabria and its possible consequences for the Hercynian orogeny in southern Europe. *Earth and Planetary Science Letters* **56**, 305–320.

Schenk V (1984) Petrology of felsic granulites, metapelites, metabasics, ultramafics, and metacarbonates from Southern Calabria (Italy): prograde metamorphism, uplift and cooling of a former lower crust. *Journal of Petrology* **25**, 255–296.

Schenk V (1990) The exposed crustal cross section of southern Calabria, Italy: structure and evolution of a segment of Hercynian crust. *Exposed cross-sections of the continental crust* **317**, 21–42.

Schulmann K, Mlčoch B and Melka R (1996) High-temperature micro-structures and rheology of deformed granite, Erzgebirge, Bohemian Massif. *Journal of Structural Geology* **18**, 719–733.

Stipp M, Stünitz H, Heilbronner R and Schmid SM (2002) The eastern Tonale fault zone: a 'natural laboratory'for crystal plastic deformation of quartz over a temperature range from 250 to 700 C. *Journal of Structural Geology* **24**, 1861–1884.

Tortorici G, Bianca M, de Guidi G, Monaco C and Tortorici L (2003) Fault activity and marine terracing in the Capo Vaticano area (southern Calabria) during the Middle-Late Quaternary. *Quaternary International* **101**, 269–278.

Vernon RH (2000) Review of microstructural evidence of magmatic and solid-state flow. *Visual Geosciences* **5**, 1–23.

Vernon RH (2018) *A Practical Guide to Rock Microstructure*. Cambridge: Cambridge University Press.

Vigneresse JA and Clemens JD (2000) Granitic magma ascent and emplacement: neither diapirism nor neutral buoyancy. *Geological Society, London, Special Publications* **174**, 1–19.

Vigneresse JL (1999) Should felsic magmas be considered as tectonic objects, just like faults or folds? *Journal of Structural Geology* **21**, 1125–1130.

Von Raumer J, Stampfli G, Borel G and Bussy F (2002) Organization of pre-Variscan basement areas at the north-Gondwanan margin. *International Journal of Earth Sciences* **91**, 35–52.

Von Raumer JF, Bussy F, Schaltegger U, Schulz B and Stampfli GM (2013) Pre-Mesozoic Alpine basements—their place in the European Paleozoic framework. *Bulletin* **125**, 89–108.

Von Raumer JF, Stampfli GM and Busy F (2003) Gondwana-derived microcontinents—the constituents of the Variscan and Alpine collisional orogens. *Tectonophysics* **365**, 7–22.

Weinberg RF, Vernon RH and Schmeling H (2021) Processes in mushes and their role in the differentiation of granitic rocks. *Earth-Science Reviews* **220**, 103665.

Whitney DL and Evans BW (2010) Abbreviations for names of rock-forming minerals. *American mineralogist* **95**, 185–187.

Žák J, Verner K, Holub FV, Kabele P, Chlupáčová M and Halodová P (2012) Magmatic to solid state fabrics in syntectonic granitoids recording early Carboniferous orogenic collapse in the Bohemian Massif. *Journal of Structural Geology* **36**, 27–42.

Zibra I, Kruhl JH, Montanini A and Tribuzio R (2012) Shearing of magma along a high-grade shear zone: Evolution of microstructures during the transition from magmatic to solid-state flow. *Journal of Structural Geology* **37**, 150–160.